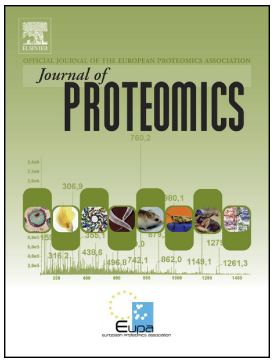

Decellularized extracellular matrix from bovine ovarian tissue maintains the protein composition of the native matrisome

Cecibel M. León-Félix, Emna Ouni, Gaëtan Herinckx, Didier Vertommen, Christiani A. Amorim, Carolina M. Lucci

PII: S1874-3919(24)00279-3

DOI: https://doi.org/10.1016/j.jprot.2024.105347

Reference: JPROT 105347

To appear in: *Journal of Proteomics*

Received date: 27 August 2024

Revised date: 15 October 2024

Accepted date: 4 November 2024

Please cite this article as: C.M. León-Félix, E. Ouni, G. Herinckx, et al., Decellularized extracellular matrix from bovine ovarian tissue maintains the protein composition of the native matrisome, *Journal of Proteomics* (2024), https://doi.org/10.1016/j.jprot.2024.105347

Decellularized extracellular matrix from bovine ovarian tissue maintains the protein composition of the native matrisome

Authors:

Cecibel M. León-Félix[a], Emna Ouni[b], Gaëtan Herinckx[c], Didier Vertommen[c], Christiani A. Amorim[d,*], Carolina M. Lucci[a,*]

Affiliations:

[a] Institute of Biological Sciences, Department of Physiology, University of Brasilia, Brasilia 70910-900, Brazil

[b] Tumor Cell Dynamics Unit, Inserm U1279, Gustave Roussy Institute, Université Paris-Saclay, Villejuif 94800, France

[c] PHOS Unit and MASSPROT Platform de Duve Institute, Université Catholique de Louvain, Brussels 1200, Belgium

[d] Pôle de Recherche en Physiopathologie de la Reproduction, Institut de Recherche Expérimentale et Clinique, Université Catholique de Louvain, Brussels 1200, Belgium

***Corresponding authors:**

Prof. Carolina M. Lucci

Address: Instituto de Biologia, Universidade de Brasília, Campus Darcy Ribeiro, Asa Norte, Brasília – DF. Brazil. 70910-900

Tel: +55 61 98581-4662

E-mail: carollucci@gmail.com

Prof. Christiani A. Amorim

Address: Pôle de Recherche en Physiopathologie de la Reproduction, Avenue Hippocrate, 54 Bte. B1.55.03 - 1200 Bruxelles, Belgique

TEL: +32 (0)2 43 61017

E-mail: christiani.amorim@uclouvain.be

Abstract

Recent approaches of regenerative reproductive medicine investigate the decellularized extracellular matrix to develop a transplantable engineered ovary (TEO). However, a full proteomic analysis is not usually performed after the decellularization process to evaluate the preservation of the extracellular matrix (ECM). In this study, the ECM of the bovine ovarian cortex was analyzed before and after decellularization using mass spectrometry and bioinformatics. A total of 155 matrisome proteins were identified in the native ECM of the bovine ovarian cortex, with 145 matrisome proteins detected in the decellularized ECM. After decellularization, only 10 matrisome proteins were lost, and notably, none belonged to the category of reproductive biological processes. Histology and histochemistry analyses were employed to assess the general morphology of both native and decellularized ECM, allowing for the identification of the most abundant ECM proteins. Moreover, our study highlighted collagen type VI alpha 3 and heparan sulfate proteoglycan 2 as the most abundant components in the bovine ovarian ECM, mirroring the composition observed in the human ovary. These findings enhance our understanding of the composition of both native and decellularized ECM, with the potential implications for the development of a TEO.

Keywords:

Matrisome, proteomics, proteins, ECM, ovary.

Significance

The significance of the present study lies on the possibility of advancing towards developing a bioengineered ovary, which is the ultimate strategy to regain fertility in women. The results demonstrate that the decellularized extracellular matrix of the bovine ovary maintains the protein composition of the native matrisome, using a recently described decellularization protocol. The decellularized matrix may serve as scaffolding for seeding ovarian stromal cells and follicles to create a bioengineered ovary, and as closer its composition is to the native matrix the better. Also, comparing the bovine ovarian matrisome, which was described for the first time here, with the human ovarian matrisome, we could see a great similarity, suggesting that the bovine ovary decellularized matrix may serve as a model for developing a human bioengineered ovary.

Introduction

In recent years, the field of regenerative medicine applied to reproduction has witnessed significant advancements, particularly in the development of new assisted reproductive technologies (ART) for infertility treatment [1]. Cancer patients undergoing chemotherapy and/or radiotherapy may experience ovarian function loss after treatment [2], making them potential candidates for ART interventions. However, individuals diagnosed with cancer at risk of ovarian metastasis [3] face challenges in accessing technologies, such as ovarian tissue cryopreservation for future autotransplantation, due to concerns about reintroducing cancerous cells [4,5]. To address these challenges, researchers are investigating the transplantable engineered ovary (TEO) as a novel approach to restore female fertility and hormonal production.

The TEO relies on the interaction between a three-dimensional structure containing isolated preantral follicles and ovarian cells, aiming to support the complete development of follicles, oocyte maturation, and the proper production of female sex hormones [6,7]. To achieve this, it is necessary to reproduce the microenvironment of a native ovarian extracellular matrix (ECM), as the ECM plays a dynamic and essential role in folliculogenesis and steroidogenesis in the ovary [8,9]. To obtain a cell-free native ECM while preserving the inherent characteristics of the ovarian tissue's ECM, decellularization techniques have been employed in ovarian tissue (for a review see Wu et al. [10]). Recently, we developed a mild decellularization protocol for the bovine ovarian cortex, which yielded a decellularized ECM (dECM) morphologically similar to the native ovarian ECM [11].

The development of a dECM from an animal model is extremely important due to the limited availability of human ovarian samples. The bovine ovary, due to its striking resemblance to the human ovary in numerous aspects [12,13], presents a viable alternative. A successfully dECM lacks nuclear material, preventing immunological reactions in the recipient [14,15]. Previous studies have demonstrated the immune compatibility of dECM derived from bovine tissues in various applications, such as bone grafting and vascular bypass surgeries for humans [16,17]. Therefore, the dECM derived from the bovine ovarian cortex holds promise as a potential scaffold for human ovarian tissue engineering.

Another important aspect to consider when using dECM from an animal model is the conservation of ECM molecules across different species, a well-documented topic in the literature [18,19]. While dECM is usually evaluated morphologically, through immunohistochemistry and scanning electron microscopy, and quantitatively, using colorimetric techniques to examine certain ECM components [20–22], these assessments may not provide a detailed understanding of the preservation of ovarian ECM components. Hence, the primary objective of this study is to undertake a thorough proteomic analysis of the bovine ovarian dECM using our recently developed decellularization protocol [11]. We hypothesize that the mild nature of our protocol will effectively preserve a substantial number of matrisome proteins, yielding a scaffold capable of fostering folliculogenesis. To this end, we will compare bovine ovarian dECM matrisome with the native counterpart.

Material and Methods

Ovarian tissue

Ovaries from bovines were collected from local slaughterhouses[1] (Frigoias and Bom Corte, Anapolis and Formosa-GO, Brazil) and transported to the laboratory in PBS at 37°C. Upon arrival, the ovaries were carefully cleaned and stored at -20°C. Prior to experimentation, the ovaries were thawed, the antral follicles were aspirated, and the epithelial and medullary layers of the ovary were meticulously removed with a scalpel. Subsequently, samples measuring 10 mm x 5 mm x 1 mm were extracted from the cortical region, weighed, and evenly distributed among control and decellularization (decell) groups.

Decellularization protocol

Samples from different baches of ovarian tissue were assigned to the decell group and underwent decellularization process as per the protocol previously described by León-Félix et al. [11]. Briefly, the tissue samples were incubated in 10 mL of 0.1% sodium dodecyl sulfate (SDS; L3771-100G, Sigma-Aldrich, St. Louis, Missouri, USA) and 0.02M sodium hydroxide (NaOH; 106467, Sigma-Aldich) in distilled water for 12 h at room temperature under constant stirring (100 rpm). Then, the samples were washed in 50 mL of distilled water for 6 h, under continuous stirring, with the water being changed every 30 min. The samples designated for the control group underwent a treatment with distilled water alone, following the same procedure as the decell group. Finally, all

[1] Ethics approval is not required for the use of bovine ovaries from slaughterhouses as stipulated in the national guidelines (CONCEA Nº 55, DE 5 DE OUTUBRO DE 2022).

samples were lyophilized and stored for subsequent analyses. Figure 1 shows the appearance of ovarian tissue following the steps of the decellularization process.

Sample preparation for mass spectrometry

Samples (n = 5 per group) from different ovaries were processed individually following the protocol established by Ouni et al. [23]. In brief, each sample was transferred to an empty 2 mL FastPrep® Lysing matrix tube (MP Biomedicals, California, USA) and covered with 100 µL of lysis buffer containing 0.2 % RapiGest SF (Water Corp, Milford, MA, USA), 300 mM NaCl, 25 mM HEPES, 0.25 mM sodium orthovanadate (81104, Alfa Aesar, Germany), 50 mM NaF (P756.1, CarlRoth, Germany), 0.25 mM Phenylmethanesulfonyl fluoride (52332, Sigma-Aldrich), 1X cOmplete, EDTA-Free protease inhibitor cocktail (11873580001, Roche, Mannheim, Germany) and 5 mM EDTA. Mechanical lysis was performed using 0.3 mm-diameter stainless steel beads (Full Moon, BioSystems, Sunnyvale, CA, USA) with homogenization carried out at 4˚C with Precellys Evolution (Bertin Technologies, Montighny-le-Breton-neux, France). The homogenate was eluted with the needle technique, as described by Ouni et al. [23], followed by centrifugation at 3000 *g* for 5 min at 4°C. The resulting eluate was then subjected to another round of centrifugation at 16,000 *g* for 30 min at 4°C to recover the supernatant. The total protein content of this fraction was quantified using the Pierce™ BCA Protein Assay Kit (23225, Thermo Scientific).

A total of 100 µg of total supernatant proteins was reduced with 5 mM 1,4-Dithiothreitol (DTT; D0632, Sigma-Aldrich), incubated for 30 min at 56°C and then alkylated with 25 mM chloroacetamide for 25 min at room temperature in the dark. Then, the proteins were precipitated using methanol-chloroform, resuspended in 50 mM TEAB (pH 8), and subjected to digestion using Lys-C/Trypsin (V507A, Thermo Scientific) at the enzyme-to-substrate ratio of 1:25 [wt/wt] overnight at 37°C. After digestion, the RapiGest SF was removed by hydrolysis, and the samples were acidified with 0.5% final TFA and incubated for 1 hour at 37°C. The resulting mixture was then centrifuged at 16,000 *g* for 10 min at 4°C and the supernatant was transferred to a new tube. The recovered peptides were quantified using the Pierce™ Quantitative Colorimetric Peptide Assay (23275, Thermo Scientific).

Liquid chromatography –tandem-mass-spectrometry

Peptides were dissolved in solvent A (0.1% TFA in 2% ACN), directly loaded onto reversed-phase pre-column (Acclaim PepMap 100, Thermo Scientific) and eluted in backflush mode. Peptide separation was performed using a reversed-phase analytical column (Acclaim PepMap RSLC, 0.075 x 250 mm, Thermo Scientific) with a linear gradient of 4%-27.5% solvent B (0.1% FA in 98% ACN) for 40 min, 27.5%-50% solvent B for 20 min, 50%-95% solvent B for 10 min and holding at 95% for the last 10 min at a constant flow rate of 300 nl/min on an Ultimate 3000 RSLC system. The peptides were analyzed by an Orbitrap Fusion Lumos tribrid mass spectrometer (ThermoFisher Scientific). The peptides were subjected to NSI source followed by tandem mass spectrometry

(MS/MS) in Fusion Lumos coupled online to the nano-LC. Intact peptides were detected in the Orbitrap at a resolution of 120,000. Peptides were selected for MS/MS using HCD setting at 30, ion fragments were detected in the Ion Trap. A data-dependent procedure that alternated between one MS scan followed by MS/MS scans was applied for 3 seconds for ions above a threshold ion count of 5.0E3 in the MS survey scan with 60.0s dynamic exclusion. The electrospray voltage applied was 2.1 kV. MS1 spectra were obtained with an AGC target of 4E5 ions and a maximum injection time of 50ms, and MS2 spectra were acquired with an AGC target of 1E4 ions and a maximum injection set to 35ms. For MS scans, the m/z scan range was 375 to 1800. The resulting MS/MS data was processed using Sequest HT search engine within Proteome Discoverer 2.5 SP1 against a *Bos taurus* protein database obtained from Uniprot. Trypsin was specified as cleavage enzyme allowing up to 2 missed cleavages, 4 modifications per peptide and up to 5 charges. Mass error was set to 10 ppm for precursor ions and 0.5 Da for-fragment ions. Oxidation on Met (+15.995 Da), was considered as variable modifications. False discovery rate (FDR) was assessed using Percolator and thresholds for protein, peptide and modification site were specified at 1%. For abundance comparison, abundance ratios were calculated by Label Free Quantification (LFQ) of the precursor intensities within Proteome Discoverer 2.5 SP1

Proteomic data and statistical analysis

All proteins identified with ≥ 2 unique peptides were compared with the human *in-silico* matrisome (http://matrisomeproject.mit.edu/). These proteins were

characterized according to Naba et al. [24,25] based on core matrisome proteins, including ECM glycoproteins, collagens and proteoglycans, as well as matrisome-associated proteins, such as ECM-affiliated proteins, ECM regulators and secreted factors, using the Matrisome Annotator (http://matrisomeproject.mit.edu/analytical-tools/matrisome-annotator/). Bioinformatic analysis was performed on each identified protein using JMP® Pro 16 Statistical Software and WebGestalt online (htt://WebGestalt.org). Furthermore, a statistical analysis, which included Pearson's correlation analysis and Student's t-distribution ($p < 0.05$), was performed using GraphPad Prism® 9 Statistical Software to quantify and compare the abundances of proteins present between both groups. If a protein was absent in one of the groups, no statistical analysis was performed on that protein.

Histological and Immunohistochemical analysis

Histological analysis was conducted on both control and decell group samples (n=5 per group). Samples were fixed in 4% paraformaldehyde, dehydrated, embedded in paraffin, and cut into 5 μm-thick sections. Sections from each sample were stained with hematoxylin-eosin (Sigma, Hannover, Germany), Masson’s trichrome and Alcian blue satin (pH 2.5) staining in order to assess the general appearance of the ovarian ECM, the content of collagen fibers and carboxylated and sulfated glycosaminoglycans, respectively.

Additional sections were used for immunohistochemical analyses. Sections were deparaffinized with Histosafe (Yvsolab SA, Beerse, Belgium) and rehydrated in alcohol. Endogenous peroxidase was blocked with 3% H_2O_2,

epitope unmasking with 0.01 M citrate buffer (0.019 M citric acid, 0.082 M sodium citrate dihydrate, and 20% Triton-X100, pH 6,) at 96°C for 75 min. Nonspecific reactions were blocked with 10% normal goat serum (NGS) and 1 % bovine serum albumin (BSA) for 30 min.

Primary rabbit antibodies used in this study included collagen type VI alpha 3 (1/100 dilution, PA549914, Thermo Fisher Scientific, Dilbeek, Belgium), elastin microfibril interfacer 1 (EMILIN-1; 1/100 dilution, HPA002822, Sigma-Aldrich), fibrilin-1 (1/100 dilution, HPA017759, Sigma-Aldrich) and elastin (1/100 dilution, PA599418, Thermo Fisher Scientific). These antibodies were diluted in TBS containing 1% NGS and 0.1% BSA, and the slides were incubated with the primary antibodies overnight at 4°C. The secondary antibodies were horseradish peroxidase (HRP)-conjugated anti-rabbit (K003, EnVision^{TM}+, Dako, Glostrup, Denmark) for 1 h at room temperature. After, the slides were treated with 3,3'-diaminobenzidine (DAB) substrate chromogen system (K3468, EnVision^{TM}+, Dako) for 15 min, followed by counterstaining with hematoxylin. Slides were mounted with DPX mounting medium. Positive controls consisting of human ovarian tissue were utilized, while negative controls were prepared without the addition of the primary antibodies.

Comparison between bovine and human ovarian cortex matrisome proteins

A comparison was made between the matrisome proteins identified in this study and those reported in humans [26,27]. Proteins were identified based on their

gene symbols informed in the UniProt proteomic database to ensure they referred to the same proteins.

Results

Quantification of proteins

The quantification of soluble proteins yielded a concentration of 3.5 ± 0.3 µg/µL (mean ± SD) in the control group (n = 5), and 2.1 ± 0.2 µg/µL (mean ± SD) in the decell group (n = 5). These results demonstrate a statistically significant difference ($p < 0.0001$) between the two groups (Fig. 2).

Total ovarian proteome analysis

Comparison of all detected proteins (unique peptides ≥ 2; FDR at 1%) with a curated *in-silico* protein set of the human matrisome obtained from the Matrisome Project (http://matrisomeproject.mit.edu/), resulted in the identification of 155 matches. The pool of matrisome proteins identified was further characterized for the control and decell groups. In the control group, a total of 155 matrisome proteins were found, consisting of 87 core matrisome proteins. Among the core matrisome proteins, 37.42% were ECM glycoproteins, 11.60% were collagens, and 7.10% were proteoglycans. Additionally, 68 matrisome-associated proteins were identified in the control group, including 21.29% ECM regulators, 17.42% ECM-affiliated proteins, and 5.16% secreted factors (Table 1). In the decell group, a total of 145 matrisome proteins were

identified, comprising 84 core matrisome proteins. Among the core matrisome proteins, 37.93% were ECM glycoproteins, 12.41% were collagens, and 7.59% were proteoglycans. Furthermore, 61 matrisome-associated proteins were found in the decell group, which included 21.38% ECM regulators, 16.55 % ECM-affiliated proteins, and 4.14% secreted factors (Table 1).

Ovarian ECM proteome map of the control and decell groups

The matrisome composition is shown in Figure 3. Proteins present in both the control and decell groups were subjected to a statistical comparison ($p < 0.05$) based on abundance (log10 [mean of each group]). Additionally, all identified proteins were ranked from highest to lowest according to their corresponding peptide spectrum matches (PSM). Following decellularization, ten proteins were found to be absent. These included three ECM glycoproteins (SPARC, homologous peroxidasin, and multimerin 2), one ECM regulator protein (procollagen-lysine,2-oxoglutarate 5-dioxygenase 3), three ECM-affiliated proteins (glypican 1, plexin A4 and plexin B1) and two secreted factors (angiopoietin-like 2 and angiopoietin-4). However, the number of collagen and proteoglycan proteins remained the same in both groups.

Top 58 detected proteins

The identification of the most abundant proteins in both the control group and decell group was pooled and ranked according to their number of PSM (Fig. 4). The most abundant proteins observed were collagen type VI, heparan sulfate

proteoglycan 2, the ECM glycoprotein Tenascin XV, the ECM-affiliated protein annexin A2 and the ECM regulator serpin H1.

Gene ontology analysis of ovarian ECM proteome of the control and decell groups

All gene symbols of each protein identified in the control and decell groups (mentioned above) were analyzed by WebGestalt online (htt://WebGestalt.org). The following criteria were selected: *Bos taurus* as the organism of interest and over-representation analysis (ORA) as the method of interest. The result was the division of proteins into 12 biological processes (Fig. 5A), 19 cellular components (Fig. 5B), and 13 molecular functions (Fig. 5C).

Histological and immunohistochemical analyses

Histological and histochemistry evaluations showed the preservation of the general morphology of ECM and the two most important groups of ECM proteins (collagen and glycoproteins) after decellularization of the bovine ovarian ECM (Fig. 6). Furthermore, immunohistochemistry analysis showed the preservation of specific proteins after decellularization: collagen type VI alpha 3, a significant member of the collagen group, as well as EMILIN-1, fibrillin-1, and elastin, which are ECM glycoproteins (Fig. 7), confirming the proteomics results.

Comparison between bovine and human ovarian cortex matrisome proteins

The proteins identified in both species are presented in Tables 2 to 7. Among the core matrisome proteins, 30 glycoproteins were common for the bovine and human ovarian matrisome, from a total of 58 glycoproteins identified in the bovine and 35 in the human. From the 17 collagens identified in the human matrisome, 13 were also identified in the bovine, and another 5 were exclusively found in the bovine. All 9 proteoglycans identified in the human ovary matrisome were shared with the bovine, with 2 more in the bovine only. Among the matrisome-associated proteins, 33 ECM regulators were identified in the bovine and 26 in the human matrisome, with 19 shared between the species. On the ECM-affiliated proteins, 27 proteins were identified on the bovine ovary, and 16 on the human ovary, with 15 shared proteins. In the secreted factors category, the bovine and human matrisome presented 8 and 11 proteins, respectively, with only 4 in common.

Discussion

The present study describes for the first time the ECM proteins from the bovine ovarian cortex. This matrisome profile serves as the foundation for evaluating a recently introduced method for decellularizin of bovine ovarian cortex using a minimum SDS concentration and incubation period [11]. Previously, we demonstrated that this optimized decellularization protocol effectively removed cellular components while preserving the structural integrity of the ovarian tissue. Here, we report that this gentle decellularization protocol retained

approximately 93.5% of the matrisome proteins, showcasing its efficacy and potential suitability for tissue engineering applications.

After analysis, we identified 155 ECM proteins before decellularization and 145 ECM proteins after decellularization. While statistical differences were observed in some proteins, the total loss after decellularization amounted to only 10 ECM proteins. Other studies described that protein levels were significantly reduced after decellularization, possibly due to more aggressive protocols using combinations of decellularizing agents (SDS, Triton X-100, NaOH and/or SDC, and DNase and/or RNase), in higher concentrations (3%, 2% and 1%) and for longer incubation periods (36-,16- and 12- hours) [14,20–22,28], proving that our decellularization method, using 0.1% SDS for 12h [11], is gentler. However, none of these works thoroughly analyzed the effect of decellularization on the ovarian ECM, especially quantitatively for each component of the ovarian ECM. The only study that evaluated the matrisome found a total of 82 proteins on the decellularized porcine ovary [29] which is much less than the 145 proteins found on the dECM on the bovine ovarian cortex, although they did not describe the proteins in the native matrix.

Prior investigations have described the matrisome composition in the native human ovarian cortex [26,27]. The total number of matrisome proteins identified in our work in the native bovine ovarian cortex (155 proteins), was greater than that described for the matrisome of the native human ovarian cortex (120 proteins - Ouni et al. [27]). Although not all proteins identified in the human ovarian cortex are expressed in the bovine ovarian cortex and vice-versa (Tables 2 to 7), there is 84% analogy between core matrisome proteins, suggesting the bovine ovary may be a good model for human ovary studies and

also the dECM from bovine ovarian cortex might be a suitable scaffold for the development of human follicles.

Besides comparing the matrisome composition before and after decellularization, our study delved into the biological and molecular functions of the ECM proteins, although the specific functions of each protein in the ovary remain to be elucidated.

Glycoproteins constituted the highest proportion of core matrisome proteins in the human ovarian cortex (28 glycoproteins - Ouni et al. [26]) and porcine dECM (36 glycoproteins - Henning et al. [29]), which is consistent with our findings. However, we identified a greater number of glycoproteins in both native (58 glycoproteins) and decellularized (55 glycoproteins) bovine ovarian cortex in comparison with those studies. For instance, tenascin C, which is involved in the process of tissue remodeling and the regulation of cell migration [30], specifically suppressing estradiol secretion from granulosa cells and androstenedione secretion from theca cells in the ovary [31]. In addition, laminin subunit gamma 3 and matrix Gla protein, which play a role in cell differentiation [30]. Notably, the most abundant glycoprotein in the bovine ovarian cortex is tenascin XB, in contrast to fibrillin-1 in the human ovarian cortex [26].

The second most abundant group of proteins in the core matrisome of the ovarian cortex consists of different types of collagens. While previous studies identified 16 types of collagens in human ovarian cortex matrisome [27] and 11 types in decellularized porcine ovary [29], we identified 18 different types of collagens in bovine ovarian cortex. Remarkably, we identified three novel collagen types (collagen type IV alpha 3 (COL4A3), collagen type IV alpha 6

(COL4A6), and collagen type V alpha 3 (COL5A3)) within the matrisome that had not been previously reported in other ovarian matrisomes. These collagens unwrap the organizing function of the ECM [30]. Moreover, COL4A3 also unwraps the function of cell signaling, namely through the collagen-activated tyrosine kinase receptor signaling pathway necessary for transcription, and COL5A3 unwraps the function of cell attachment to the ECM via adhesion molecules [30]. Furthermore, the most abundant collagen in the bovine ovarian cortex was collagen type VI alpha 3 (COL6A3), consistent with the human ovarian cortex [26].

Finally, the lowest percentage of proteins identified in the core matrisome are proteoglycans. Previous studies reported the identification of 8 types of proteoglycans [26,29], whereas we identified 11 different types of proteoglycans. Among these, asporin (ASPN) and hyaluronan and proteoglycan link protein 3 (HAPLN3) were novel findings in the ovarian matrisome. ASPN negatively regulates the transforming growth factor beta receptor signaling pathway [30] and is implicated in fibrosis regulation [32], while HAPLN3 is involved in cell adhesion [30]. Furthermore, the most abundant proteoglycan in the bovine ovarian cortex was heparan sulfate proteoglycan 2, consistent with human ovarian cortex [26].

Regarding matrisome-associated proteins, previous studies reported the identification of 47 matrisome-associated proteins in the human ovarian cortex [27] and 32 proteins in decellularized porcine ovary [29]. However, our study yielded 68 in the native bovine ovarian cortex and 61 proteins in its decellularized version. Additionally, we discovered novel matrisome-associated proteins that had not been previously described. For example, 72 kDa

collagenase type IV is involved in ECM remodeling function and is associated with ovarian cancer metastasis [33,34]. C-type lectin domain containing 11A stimulates female germ line cell proliferation [35], and frizzled-related protein activates primordial follicle granulosa cells [36]. Similar to the human ovarian cortex [26], annexin A2 was identified as the most abundant ECM-affiliated protein in the bovine ovarian cortex. Moreover, the most abundant proteins in the categories of ECM regulators and secretory factors in the bovine ovarian cortex were serpin family H member 1 and protein S100-A16, respectively, contrasting with serpin family A member 1 and protein S100-A11 in the human ovarian cortex [26].

From those 10 proteins that were completely lost after the decellularization process, 3 belonged to the core matrisome category and 7 to the matrisome-associated proteins, but none of them belonged to the reproductive biological process category. These proteins participate in molecular functions related to ion binding, protein binding, transferase activity, carbohydrate binding, and hydrolase activity. One example of these proteins is procollagen-lysine, 2-oxoglutarate 5-dioxygenase 3, which plays a role in collagen synthesis in the ECM. This protein encodes the enzyme lysyl hydroxylase, which catalyzes the hydroxylation of hydroxyproline, allowing the formation of procollagen before its final conversion into collagen [37]. Other relevant examples are plexin-A4 and B1, which act as transmembrane receptors for signaling proteins of the semaphorin family. Both proteins form complexes that participate in signal transduction, angiogenesis, and immune response [38,39]. Nevertheless, it is important to note that the loss of some proteins from the ECM after the decellularization process may not significantly affect the tissue's physiology,

because the functions of ECM are not exclusively carried out by a single protein. Even though, it is not clear how the slight modification of the ECM composition after the decellularization process will affect its functions. What we can affirm is that our decellularization method is quite conservative, providing a dECM that closely resembles the native ECM.

The proteins preserved in the dECM play various functions in tissues, although their interactions within the physiological dynamics of the ovary have not yet been fully described. Overall, the different types of collagen present in the dECM play an essential role in maintaining structural stability and elasticity, preserving the three-dimensional architecture of the tissue and providing support for the ovarian follicles during folliculogenesis. An example is collagen type VI whose interaction with theca cells during the transition from secondary to preovulatory follicle promotes follicular adhesion [40]. Furthermore, it has been shown that collagen is crucial for *in vitro* folliculogenesis, promoting the development of immature follicles towards ovulation [41]. The preservation of glycoproteins in the dECM not only ensures structural stability but also facilitates cell-cell and cell-matrix communication. For example, tenascin, retained in the dECM, contributes to maintaining the three-dimensional structure of the follicle during folliculogenesis and facilitates its mobility throughout development [42]. Similarly, transforming growth factor-beta-induced protein ig-h3, also present in the dECM, promotes ovarian cell motility and increases cell-cell adhesion in *in vitro* cultures [43]. Retened proteoglycans promote cellular signaling by regulating growth factors. One example is decorin, which modulates the activity of several epidermal growth factors through the regulation of intracellular Ca^{2+} levels, thereby reducing apoptosis in luteal cells

[44], prolonging the lifespan of the corpus luteum and, consequently, progesterone production. Also, matrix metalloproteinases (MMP2 and MMP14), both present in the dECM, plays a key role in ovarian remodeling, facilitating follicular growth, ovulation, and luteolysis [45]. These enzymes are induced by SPARC, a proteoglycan also preserved in the dECM, during these physiological events [45]. It is also worth noting that SPARC is involved in angiogenesis during corpus luteum formation [46].

The proteins preserved in the dECM might positively affect the scaffold's performance when used in tissue engineering by enhancing the scaffold’s ability to support cell attachment, proliferation, and follicle development, as exemplified above. Together, the preserved core-matrisome and matrisome-associated proteins would support cell adhesion and proliferation, as well as facilitate follicular development by maintaining its three-dimensional structure and allowing matrix remodeling during follicular growth. In general, the ECM proteins participate in a dynamic interaction mediated by biochemical signals between the ovarian follicles and the ovarian ECM. This communication is essential for the recruitment and follicular dominance phase, as well as for oocyte maturation and the production of the required sex hormones to carry out these processes. Moreover, the connection between both ovarian components is also necessary for new blood vessel formation in the ECM and constant ECM remodeling. It is important to note that the decrease in abundance and loss of some proteins from ECM after the decellularization process may not significantly affect the various processes occurring during folliculogenesis and steroidogenesis, because usually the functions of ECM are not exclusively carried out by a single protein, instead several proteins play similar roles.

Moreover, decellularized ECM can be enriched with proteins whose abundance decreased or were lost during the decellularization process.

Conclusion

This study offers a comprehensive characterization and comparison of ECM proteins in the native and decellularized bovine ovarian cortex. The results proved that the decellularization method used is quite conservative, providing a dECM very similar to the native ECM. The findings also contribute to a better understanding of the roles played by ECM proteins in folliculogenesis and steroidogenesis in the ovary. Additionally, we identified a high similarity in the major ECM proteins between bovine and human ovaries, supporting that the bovine ovarian dECM holds potential for utilization in the development of an ovarian tissue engineering approach for women.

Funding

The funding for this study was supported by grants from the *Coordenação de Aperfeiçoamento de Pessoal de Nível Superior - Brasil* (CAPES) (Finance Code 001), Erasmus+ Dimension internationale (convention grant no. DS/VM/CAI45-1011 awarded to C.A.A., Ph. D. scholarship awarded to C.M.L.F.) and Southeast Asia – Europe Joint Funding Scheme for Research and Innovation (FNRS PINT, convention grant no. R.8002.21 awarded to C.A.A., Ph. D. scholarship awarded to C.M.L.F.).

CRediT authorship contribution statement

Cecibel M. León-Félix: Conceptualization, Methodology, Formal analysis, Investigation, Writing - original draft, Writing - Review & Editing. **Emna Ouni:** Methodology; Writing - Review & Editing. **Gaëtan Herinckx:** Methodology, Writing - Review & Editing. **Didier Vertommen:** Methodology, Resources, Writing - Review & Editing. **Christiani A. Amorim:** Resources, Writing - Review & Editing, Supervision, Funding acquisition. **Carolina M. Lucci:** Conceptualization, Methodology, Resources, Writing - Review & Editing, Supervision and Funding acquisition.

Declaration of competing interest

The authors state that they have no known conflicting financial interests or personal relationships that could have influenced the work presented in this paper.

Data availability

The mass spectrometry proteomics data have been deposited to the ProteomeXchange Consortium via the PRIDE (http://www.ebi.ac.uk/pride/) partner repository with the dataset identifier PXD052258 and 10.6019/PXD052258.

Acknowledgments

We thank EMBRAPA-CENARGEN for donating the bovine ovaries, especially Nayara Ribeiro Kussano and Ligiane de Oliveira Leme.

References

[1] F. Zegers-Hochschild, G.D. Adamson, J. de Mouzon, O. Ishihara, R. Mansour, K. Nygren, E. Sullivan, S. van der Poel, The International Committee for Monitoring Assisted Reproductive Technology (ICMART) and the World Health Organization (WHO) Revised Glossary on ART Terminology, 2009, Human Reproduction 24 (2009) 2683–2687. https://doi.org/10.1093/humrep/dep343.

[2] T. Maltaris, R. Seufert, F. Fischl, M. Schaffrath, K. Pollow, H. Koelbl, R. Dittrich, The effect of cancer treatment on female fertility and strategies for preserving fertility, European Journal of Obstetrics & Gynecology and Reproductive Biology 130 (2007) 148–155. https://doi.org/10.1016/j.ejogrb.2006.08.006.

[3] J. Donnez, M.-M. Dolmans, A. Pellicer, C. Diaz-Garcia, M. Sanchez Serrano, K.T. Schmidt, E. Ernst, V. Luyckx, C.Y. Andersen, Restoration of ovarian activity and pregnancy after transplantation of cryopreserved ovarian tissue: a review of 60 cases of reimplantation, Fertil Steril 99 (2013) 1503–1513. https://doi.org/10.1016/j.fertnstert.2013.03.030.

[4] M. Sonmezer, K. Oktay, Orthotopic and heterotopic ovarian tissue transplantation, Best Pract Res Clin Obstet Gynaecol 24 (2010) 113–126. https://doi.org/10.1016/j.bpobgyn.2009.09.002.

[5] J. Donnez, M.-M. Dolmans, Fertility Preservation in Women, New England Journal of Medicine 377 (2017) 1657–1665. https://doi.org/10.1056/NEJMra1614676.

[6] C.A. Amorim, A. Shikanov, The Artificial Ovary: Current Status and Future Perspectives, Future Oncology 12 (2016) 2323–2332. https://doi.org/10.2217/fon-2016-0202.

[7] M.-M. Dolmans, C.A. Amorim, FERTILITY PRESERVATION: Construction and use of artificial ovaries, Reproduction 158 (2019) F15–F25. https://doi.org/10.1530/REP-18-0536.

[8] R.J. Rodgers, H.F. Irving-Rodgers, D.L. Russell, Extracellular matrix of the developing ovarian follicle, Reproduction-Cambrige 126 (2003) 415–424.

[9] T.K. Woodruff, L.D. Shea, The Role of the Extracellular Matrix in Ovarian Follicle Development, Reproductive Sciences 14 (2007) 6–10. https://doi.org/10.1177/1933719107309818.

[10] T. Wu, K.-C. Huang, J.-F. Yan, J.-J. Zhang, S.-X. Wang, Extracellular matrix-derived scaffolds in constructing artificial ovaries for ovarian failure: a systematic methodological review, Hum Reprod Open 2023 (2023). https://doi.org/10.1093/hropen/hoad014.

[11] C.M. León-Félix, A.Q. Maranhão, C.A. Amorim, C.M. Lucci, Optimizing Decellularization of Bovine Ovarian Tissue: Toward a Transplantable Artificial Ovary Scaffold with Minimized Residual Toxicity and Preserved Extracellular Matrix Morphology, Cells Tissues Organs (2024) 1–11. https://doi.org/10.1159/000537838.

[12] G.P. Adams, R.A. Pierson, Bovine model for study of ovarian follicular dynamics in humans, Theriogenology 43 (1995) 113–120. https://doi.org/10.1016/0093-691X(94)00015-M.

[13] P.S. Malhi, G.P. Adams, J. Singh, Bovine Model for the Study of Reproductive Aging in Women: Follicular, Luteal, and Endocrine Characteristics1, Biol Reprod 73 (2005) 45–53. https://doi.org/10.1095/biolreprod.104.038745.

[14] T. Wu, Y.-Y. Gao, X.-N. Tang, J.-J. Zhang, S.-X. Wang, Construction of Artificial Ovaries with Decellularized Porcine Scaffold and Its Elicited Immune Response after Xenotransplantation in Mice, J Funct Biomater 13 (2022) 165. https://doi.org/10.3390/jfb13040165.

[15] T. Talaei-Khozani, A. Yaghoubi, An overview of post transplantation events of decellularized scaffolds, Transpl Immunol 74 (2022) 101640. https://doi.org/10.1016/j.trim.2022.101640.

[16] C. Gardin, S. Ricci, L. Ferroni, R. Guazzo, L. Sbricoli, G. De Benedictis, L. Finotti, M. Isola, E. Bressan, B. Zavan, Decellularization and Delipidation Protocols of Bovine Bone and Pericardium for Bone Grafting and Guided Bone Regeneration Procedures, PLoS One 10 (2015) e0132344. https://doi.org/10.1371/journal.pone.0132344.

[17] I. Arhuidese, T. Reifsnyder, T. Islam, O. Karim, B. Nejim, T. Obeid, U. Qazi, M. Malas, Bovine carotid artery biologic graft outperforms expanded polytetrafluoroethylene for hemodialysis access, J Vasc Surg 65 (2017) 775–782. https://doi.org/10.1016/j.jvs.2016.10.080.

[18] M.P. Bernard, M.L. Chu, J.C. Myers, F. Ramirez, E.F. Eikenberry, D.J. Prockop, Nucleotide sequences of complementary deoxyribonucleic acids for the pro.alpha.1 chain of human type I procollagen. Statistical evaluation of structures that are conserved during evolution, Biochemistry 22 (1983) 5213–5223. https://doi.org/10.1021/bi00291a023.

[19] C.D. Constantinou, S.A. Jimenez, Structure of cDNAs Encoding the Triple-Helical Domain of Murine α2 (VI) Collagen Chain and Comparison to Human and Chick Homologues. Use of Polymerase Chain Reaction and Partially Degenerate Oligonucleotides for Generation of Novel cDNA Clones, Matrix 11 (1991) 1–9. https://doi.org/10.1016/S0934-8832(11)80221-0.

[20] W.-Y. Liu, S.-G. Lin, R.-Y. Zhuo, Y.-Y. Xie, W. Pan, X.-F. Lin, F.-X. Shen, Xenogeneic Decellularized Scaffold: A Novel Platform for Ovary Regeneration, Tissue Eng Part C Methods 23 (2017) 61–71. https://doi.org/10.1089/ten.tec.2016.0410.

[21] A.B. Alshaikh, A.M. Padma, M. Dehlin, R. Akouri, M.J. Song, M. Brännström, M. Hellström, Decellularization of the mouse ovary: comparison of different scaffold generation protocols for future ovarian bioengineering, J Ovarian Res 12 (2019) 58. https://doi.org/10.1186/s13048-019-0531-3.

[22] F. Eivazkhani, N.S. Abtahi, S. Tavana, L. Mirzaeian, F. Abedi, B. Ebrahimi, L. Montazeri, M.R. Valojerdi, R. Fathi, Evaluating two ovarian decellularization methods in three species, Materials Science and Engineering: C 102 (2019) 670–682. https://doi.org/10.1016/j.msec.2019.04.092.

[23] E. Ouni, S.P. dit Ruys, M.-M. Dolmans, G. Herinckx, D. Vertommen, C.A. Amorim, Divide-and-Conquer Matrisome Protein (DC-MaP) Strategy: An MS-Friendly Approach to Proteomic Matrisome Characterization, Int J Mol Sci 21 (2020) 9141. https://doi.org/10.3390/ijms21239141.

[24] A. Naba, K.R. Clauser, S. Hoersch, H. Liu, S.A. Carr, R.O. Hynes, The Matrisome: In Silico Definition and In Vivo Characterization by Proteomics of Normal and Tumor Extracellular Matrices, Molecular & Cellular Proteomics 11 (2012) M111.014647. https://doi.org/10.1074/mcp.M111.014647.

[25] A. Naba, K.R. Clauser, H. Ding, C.A. Whittaker, S.A. Carr, R.O. Hynes, The extracellular matrix: Tools and insights for the “omics” era, Matrix Biology 49 (2016) 10–24. https://doi.org/10.1016/j.matbio.2015.06.003.

[26] E. Ouni, D. Vertommen, M.C. Chiti, M.-M. Dolmans, C.A. Amorim, A Draft Map of the Human Ovarian Proteome for Tissue Engineering and Clinical Applications, Molecular & Cellular Proteomics 18 (2019) S159–S173. https://doi.org/10.1074/mcp.RA117.000469.

[27] E. Ouni, V. Nedbal, M. Da Pian, H. Cao, K.T. Haas, A. Peaucelle, O. Van Kerk, G. Herinckx, E. Marbaix, M.-M. Dolmans, T. Tuuri, M. Otala, C.A. Amorim, D. Vertommen, Proteome-wide and matrisome-specific atlas of

the human ovary computes fertility biomarker candidates and open the way for precision oncofertility, Matrix Biology 109 (2022) 91–120. https://doi.org/10.1016/j.matbio.2022.03.005.

[28] M.J. Buckenmeyer, M. Sukhwani, A. Iftikhar, A.L. Nolfi, Z. Xian, S. Dadi, Z.W. Case, S.R. Steimer, A. D'Amore, K. Orwing, B.N. Brown, Bioengineering an in situ ovary (ISO) for fertility preservation, BioRxiv (2020) 01. https://doi.org/10.1101/2020.01.03.893941.

[29] N.F. Henning, R.D. LeDuc, K.A. Even, M.M. Laronda, Proteomic analyses of decellularized porcine ovaries identified new matrisome proteins and spatial differences across and within ovarian compartments, Sci Rep 9 (2019) 20001. https://doi.org/10.1038/s41598-019-56454-3.

[30] The UniProt Consortium, UniProt: the Universal Protein Knowledgebase in 2023, Nucleic Acids Research 51 (2023) D523–D531.

[31] M. Samir, D.S. Mattar, P.G. Knight, Role of Extra Cellular Matrix Glycoprotein Tenascin C (TNC) in Ovarian Steroidogenesis and Tissue Remodelling in the Bovine Ovary, Can J Diabetes 39 (2015) 538. https://doi.org/10.1016/j.jcjd.2015.09.047.

[32] Y. Yang, P. Liu, R. Teng, F. Liu, C. Zhang, X. Lu, Y. Ding, Integrative bioinformatics analysis of potential therapeutic targets and immune infiltration characteristics in dilated cardiomyopathy, Ann Transl Med 10 (2022) 348–348. https://doi.org/10.21037/atm-22-732.

[33] J. Planagumà, M. Liljeström, F. Alameda, R. Bützow, I. Virtanen, J. Reventós, M. Hukkanen, Matrix metalloproteinase-2 and matrix metalloproteinase-9 codistribute with transcription factors RUNX1/AML1

and ETV5/ERM at the invasive front of endometrial and ovarian carcinoma☆, Hum Pathol 42 (2011) 57–67. https://doi.org/10.1016/j.humpath.2010.01.025.

[34] H. Jia, Q. Zhang, F. Liu, D. Zhou, Prognostic value of MMP-2 for patients with ovarian epithelial carcinoma: a systematic review and meta-analysis, Arch Gynecol Obstet 295 (2017) 689–696. https://doi.org/10.1007/s00404-016-4257-9.

[35] F. Li, X. Hu, J. Wu, Daidzein Activates Akt Pathway to Promote the Proliferation of Female Germline Stem Cells through Upregulating Clec11a, Stem Cell Rev Rep 18 (2022) 3021–3032. https://doi.org/10.1007/s12015-022-10394-0.

[36] E.A. Ford, E.R. Frost, E.L. Beckett, S.D. Roman, E.A. McLaughlin, J.M. Sutherland, Transcriptomic profiling of neonatal mouse granulosa cells reveals new insights into primordial follicle activation, Biol Reprod 106 (2022) 503–514. https://doi.org/10.1093/biolre/ioab193.

[37] Y. Qi, R. Xu, Roles of PLODs in Collagen Synthesis and Cancer Progression, Front Cell Dev Biol 6 (2018). https://doi.org/10.3389/fcell.2018.00066.

[38] B. Kigel, N. Rabinowicz, A. Varshavsky, O. Kessler, G. Neufeld, Plexin-A4 promotes tumor progression and tumor angiogenesis by enhancement of VEGF and bFGF signaling, Blood 118 (2011) 4285–4296. https://doi.org/10.1182/blood-2011-03-341388.

[39] H. Takamatsu, A. Kumanogoh, Diverse roles for semaphorin−plexin signaling in the immune system, Trends Immunol 33 (2012) 127–135. https://doi.org/10.1016/j.it.2012.01.008.

[40] M. Iwahashi, Y. Muragaki, A. Ooshima, R. Nakano, Type VI collagen expression during growth of human ovarian follicles, Fertil Steril 74 (2000) 343–347. https://doi.org/10.1016/S0015-0282(00)00618-X.

[41] S. Joo, S.-H. Oh, S. Sittadjody, E.C. Opara, J.D. Jackson, S.J. Lee, J.J. Yoo, A. Atala, The effect of collagen hydrogel on 3D culture of ovarian follicles, Biomedical Materials 11 (2016) 065009. https://doi.org/10.1088/1748-6041/11/6/065009.

[42] K. Yasuda, E. Hagiwara, A. Takeuchi, C. Mukai, C. Matsui, A. Sakai, S. Tamotsu, Changes in the Distribution of Tenascin and Fibronectin in the Mouse Ovary During Folliculogenesis, Atresia, Corpus Luteum Formation and Luteolysis, Zoolog Sci 22 (2005) 237–245. https://doi.org/10.2108/zsj.22.237.

[43] M.P. Ween, N.A. Lokman, P. Hoffmann, R.J. Rodgers, C. Ricciardelli, M.K. Oehler, Transforming growth factor-beta-induced protein secreted by peritoneal cells increases the metastatic potential of ovarian cancer cells, Int J Cancer 128 (2011) 1570–1584. https://doi.org/10.1002/ijc.25494.

[44] M. Adam, S. Saller, S. Strobl, J.D. Hennebold, G.A. Dissen, S.R. Ojeda, R.L. Stouffer, D. Berg, U. Berg, A. Mayerhofer, Decorin is a part of the ovarian extracellular matrix in primates and may act as a signaling molecule, Human Reproduction 27 (2012) 3249–3258. https://doi.org/10.1093/humrep/des297.

[45] G. Levin, T.M. Coelho, N.G. Nóbrega, M. Trombetta-Lima, M.C. Sogayar, A.C.O. Carreira, Spatio-temporal expression profile of matrix metalloproteinase (Mmp) modulators Reck and Sparc during the rat ovarian dynamics, Reproductive Biology and Endocrinology 16 (2018) 116. https://doi.org/10.1186/s12958-018-0422-2.

[46] P. Bagavandoss, E.H. Sage, R.B. Vernon, Secreted Protein, Acidic and Rich in Cysteine (SPARC) and Thrombospondin in the Developing Follicle and Corpus Luteum of the Rat, Journal of Histochemistry & Cytochemistry 46 (1998) 1043–1049. https://doi.org/10.1177/002215549804600908.

Table 1. Matrisome protein categories in the native (control group) and decell bovine ovarian tissue (decell group).

	Core matrisome			Matrisome-associated			
Group	**ECM glycoproteins**	**Collagens**	**Proteoglycans**	**ECM regulators**	**ECM-affiliated proteins**	**Secreted factors**	Total
Control	58	18	11	33	27	8	155
Decell	55	18	11	31	24	6	145

Table 2. Ovarian matrisome of glycoproteins in native bovine and native human cortices.

Protein name	Bovine	Human
Adiponectin (ADIPOQ)	x	
Adipocyte enhancer-binding protein 1 (AEBP1)	x	x[2]
Agrin (AGRN)	x	x[2]
Cartilage intermediate layer protein 2 (CILP2)		x[1]
Cochlin (COCH)	x	
Dermatopontin (DPT)	x	x[1,2]

EGF-containing fibulin-like extracellular matrix protein 1 (EFEMP1)	x	x[1,2]
EGF-containing fibulin-like extracellular matrix protein 2 (EFEMP2)	x	
EGF-like, fibronectin Type III and laminin G domains (EGFLAM)	x	
Elastin microfibril interfacer 1 (EMILIN1)	x	x[1,2]
Elastin microfibril interfacer 2 (EMILIN2)	x	
Extracellular matrix protein 1 (ECM1)	x	
Extracellular matrix protein 2 (ECM2)	x	
Fibrillin 1 (FBN1)	x	x[1,2]
Fibrinogen alpha chain (FGA)	x	x[1,2]
Fibrinogen beta chain (FGB)	x	x[1,2]
Fibrinogen gamma chain (FGG)	x	x[1,2]
Fibrinogen-like 2 (FGL2)	x	
Fibronectin 1 (FN1)	x	x[1,2]
Fibulin 5 (FBLN5)	x	x[1,2]
Fibulin-1 (FBLN1)	x	x[2]
Insulin-like growth factor-binding protein acid labile subunit (IGFALS)		x[1]
Isoform 3 of Tubulointerstitial nephritis antigen-like (TINAGL1)		x[1]
Lactadherin (MFGE8)	x	
Laminin subunit alpha 1 (LAMA1)	x	
Laminin subunit alpha 2 (LAMA2)	x	x[1]
Laminin subunit alpha 4 (LAMA4)	x	x[1,2]
Laminin subunit alpha 5 (LAMA5)	x	x[1,2]
Laminin subunit beta 1 (LAMB1)	x	x[1,2]
Laminin subunit beta 2 (LAMB2)	x	x[1,2]
Laminin subunit gamma 1 (LAMC1)	x	x[1,2]
Laminin subunit gamma 3 (LAMC3)	x	

Latent transforming growth factor beta binding protein 1 (LTBP1)	x	
Latent-transforming growth factor beta-binding protein 4 (LTBP4)	x	
Matrilin 2 (MATN2)	x	
Matrix Gla protein (MGP)	x	
Microfibrillar-associated protein 2 (MFAP2)		x[1]
Microfibrillar-associated protein 4 (MFAP4)	x	x[1]
Multimerin 2 (MMRN2)	x	
Netrin G2 (NTNG2)	x	
Nidogen 1 (NID1)	x	x[1,2]
Nidogen 2 (NID2)	x	x[1,2]
Periostin (POSTN)	x	x[2]
Peroxidasin homolog (PXDN)	x	
Procollagen C-endopeptidase enhancer (PCOLCE)	x	x[1]
SPARC	x	x[2]
SPARC like 1 (SPARCL1)	x	
Spondin 1 (SPON1)	x	
Sushi-repeat-containing protein, X-linked (SRPX)	x	
Sushi repeat containing protein, X-linked 2 (SRPX2)	x	
Target of Nesh-SH3 (ABI3BP)		x[2]
Tenascin C (TNC)	x	
Tenascin XB (TNXB)	x	x[1,2]
Thrombospondin 1 (THBS1)	x	x[1,2]
Transforming growth factor beta induced (TGFBI)	x	x[1,2]
Tubulointerstitial nephritis antigen like 1 (TINAGL1)	x	
Vitronectin (VTN)	x	x[1,2]
Von Willebrand factor (VWF)	x	x[1]
Von Willebrand factor A domain containing 1 (VWA1)	x	
Von Willebrand factor A domain containing 5A (VWA5A)	x	
Zona pellucida sperm-binding protein 2 (ZP2)	x	
Zona pellucida sperm-binding protein 3 (ZP3)	x	

Zona pellucida sperm-binding protein 4 (ZP4)	x	x[2]

[1] = Ouni et al. 2019, [2] = Ouni et al. 2022.

Table 3. Ovarian matrisome of collagens in native bovine and native human cortices.

Protein name	Bovine	Human
Collagen type I alpha 1 chain (COL1A1)	x	x[1,2]
Collagen type I alpha 2 chain (COL1A2)	x	x[1,2]
Collagen type II alpha 1 chain (COL2A1)		x[2]
Collagen type III alpha 1 chain (COL3A1)	x	x[2]
Collagen type IV alpha 1 chain (COL4A1)	x	x[1,2]
Collagen type IV alpha 2 chain (COL4A2)	x	x[1,2]
Collagen type IV alpha 3 chain (COL4A3)	x	
Collagen type IV alpha 6 chain (COL4A6)	x	
Collagen type V alpha 1 chain (COL5A1)	x	x[2]
Collagen type V alpha 2 chain (COL5A2)	x	x[2]
Collagen type V alpha 3 chain (COL5A3)	x	
Collagen type VI alpha 1 chain (COL6A1)	x	x[1,2]
Collagen type VI alpha 2 chain (COL6A2)	x	x[1,2]
Collagen type VI alpha 3 chain (COL6A3)	x	x[1,2]
Collagen type VI alpha 5 chain (COL6A5)	x	
Collagen type VI alpha 6 chain (COL6A6)		x[2]
Collagen type VIII alpha 1 chain (COL8A1)		x[1]
Collagen type XII alpha 1 chain (COL12A1)	x	x[1,2]
Collagen type XIV alpha 1 chain (COL14A1)	x	x[1,2]
Collagen type XV alpha 1 chain (COL15A1)	x	
Collagen type XVI alpha 1 chain (COL16A1)		x[2]
Collagen type XVIII alpha 1 chain (COL18A1)	x	x[1,2]

[1] = Ouni et al. 2019, [2] = Ouni et al. 2022.

Table 4. Ovarian matrisome of proteoglycans in native bovine and native human cortices.

Protein name	Bovine	Human
Asporin (ASPN)	x	
Biglycan (BGN)	x	x[2]
Decorin (DCN)	x	x[1,2]
Fibromodulin (FMOD)	x	x[1,2]
Heparan sulfate proteoglycan 2 (HSPG2)	x	x[1,2]
Hyaluronan and proteoglycan link protein 3 (HAPLN3)	x	
Lumican (LUM)	x	x[1,2]
Osteoglycin (OGN)	x	x[1,2]
Podocan (PODN)	x	x[1]
Proline and arginine rich leucin rich repeat protein (PRELP)	x	x[1,2]
Versican (VCAN)	x	x[2]

[1] = Ouni et al. 2019, [2] = Ouni et al. 2022.

Table 5. Ovarian matrisome of ECM regulators in native bovine and native human cortices.

Protein name	Bovine	Human
ADAM metallopeptidase domain 10 (ADAM10)	x	
Alpha-1-microglobulin (AMBP)		x[1,2]
Alpha-2-macroglobulin (A2M)	x	x[1,2]
Angiotensinogen (AGT)		x[1,2]
Cathepsin B (CTSB)		x[1]
Cathepsin D (CTSD)	x	x[1,2]

Cathepsin Z (CTSZ)		x[2]
CD109 molecule (CD109)	x	
Coagulation factor II (F2)	x	x[2]
Coagulation factor X (F10)	x	
Cystatin B (CSTB)	x	x[1,2]
Histidine-rich glycoprotein (HRG)	x	x[1,2]
HTRA serine protease 1 (HTRA1)	x	
Hyaluronoglucosaminidase 2 (HYAL2)	x	
Inter-alpha-trypsin inhibitor heavy chain H1 (ITIH1)	x	x[1,2]
Inter-alpha-trypsin inhibitor heavy chain H2 (ITIH2)	x	x[1]
Inter-alpha-trypsin inhibitor heavy chain H4 (ITIH4)	x	x[1,2]
Inter-alpha-trypsin inhibitor heavy chain H5 (ITIH5)	x	
Kininogen 1 (KNG1)	x	x[2]
Matrix metalloproteinase 14 (MMP14)	x	
Plasminogen (PLG)	x	x[1,2]
Procollagen-lysine 1,2-oxoglutarate 5-dioxygenase 1 (PLOD1)	x	
Procollagen-lysine,2-oxoglutarate 5-dioxygenase 3 (PLOD3)	x	
Prolyl 4-hydroxylase subunit alpha-1 (P4HA1)	x	
Protein-glutamine gamma-glutamyltransferase 2 (TGM2)	x	
Serpin peptidase inhibitor, clade A, member 1 (SERPINA1)	x	x[1,2]
Serpin peptidase inhibitor, clade A, member 3 (SERPINA3)		x[1,2]
Serpin peptidase inhibitor, clade A, member 4 (SERPINA4)		x[1]
Serpin peptidase inhibitor, clade A, member 5 (SERPINA5)	x	
Serpin peptidase inhibitor, clade B, member 1 (SERPINB1)		x[1,2]
Serpin peptidase inhibitor, clade B, member 6 (SERPINB6)	x	x[1,2]

Serpin peptidase inhinitor, clade C, member 1 (SERPINC1)	x	x[1,2]
Serpin peptidase inhinitor, clade D, member 1 (SERPIND1)	x	x[1,2]
Serpin peptidase inhibitor, clade E, member 2 (SERPINE2)	x	x[1]
Serpin peptidase inhibitor, clade F, member 1 (SERPINF1)	x	x[1,2]
Serpin peptidase inhibitor, clade F, member 2 (SERPINF2)	x	x[1,2]
Serpin peptidase inhibitor, clade G, member 1 (SERPING1)	x	x[1,2]
Serpin peptidase inhibitor, clade H, member 1 (SERPINH1)	x	x[1,2]
Sulfatase 2 (SULF2)	x	
72 kDa type IV collagenase (MMP2)	x	

[1] = Ouni et al. 2019, [2] = Ouni et al. 2022.

Table 6. Ovarian matrisome of ECM-affiliated in native bovine and native human cortices.

Protein name	Bovine	Human
Annexin A1 (ANXA1)	x	x[1,2]
Annexin A2 (ANXA2)	x	x[1.2]
Annexin A3 (ANXA3)	x	
Annexin A4 (ANXA4)	x	x[1,2]
Annexin A5 (ANXA5)		x[1,2]
Annexin A6 (ANXA6)	x	x[1,2]
Annexin A7 (ANXA7)	x	x[1,2]
Annexin A11 (ANXA11)	x	x[1,2]

C1QTNF5 protein (C1QTNF5)	x	
Chondroitin sulfate proteoglycan 4 (CSPG4)	x	
Collectin 12 (COLEC12)	x	
Complement C1q subcomponent subunit B (C1QB)	x	
Complement componet 1 (C1QC)	x	
C-type lectin domain containing 11A (CLEC11A)	x	
C-type lectin domain family 3 (CLEC3B)	x	x[1,2]
Galectin-1 (LGALS1)	x	x[1,2]
Galectin-3 (LGALS3)	x	x[1,2]
Galectin 9 (LGALS9)	x	
Glypican 1 (GPC1)	x	x[2]
Glypican 5 (GPC5)	x	
Glypican 6 (GPC6)	x	x[2]
Hemopexin (HPX)	x	x[1,2]
Lectin, mannose binding, 1 (LMAN1)	x	x[2]
Plexin A4 (PLXNA4)	x	
Plexin B1 (PLXNB1)	x	
Plexin domain-containing protein 2 (PLXDC2)	x	
Plexin-B2 (PLXNB2)	x	x[1,2]
Syndecan (SDC2)	x	x[2]

[1] = Ouni et al. 2019, [2] = Ouni et al. 2022.

Table 7. Ovarian matrisome of secreted factors in native bovine and native human cortices.

Protein name	Bovine	Human
Angiopoietin like 2 (ANGPTL2)	x	
Angiopoietin-4 (ANGPT4)	x	
Filaggrin (FLG)		x[2]
Frizzled-related protein (FRZB)	x	

Hornerin (HRNR)		x[2]
Host cell factor 1 (HCFC1)	x	x[1]
Protein S100-A6 (S100A6)		x[1,2]
Protein S100-A7 (S100A7)		x[2]
Protein S100-A8 (S100A8)		x[2]
Protein S100-A9 (S100A9)		x[2]
Protein S100-A10 (S100A10)	x	x[2]
Protein S100-A11 (S100A11)		x[1]
Protein S100-A13 (S100A13)	x	x[1,2]
Protein S100-A14 (S100A14)	x	
Protein S100-A16 (S100A16)	x	x[2]

[1] = Ouni et al. 2019, [2] = Ouni et al. 2022.

Figure captions

Fig. 1. Bovine ovaries appearance following the steps of the decellularization protocol. First bovine ovaries had antral follicles aspirated and were cut in half (A), next the ovarian capsule (A) and medullary region (B) were removed. Then, the cleaned half-ovary was placed in a tissue slicer matrix where 1 mm thick slices were cut with a sharp blade (C), which were subsequently placed on a glass plate over paper with a previously delimited rectangle (10 mm x 5 mm) to adjust the final size of the sample (D). After the decellularization protocol, the tissue had a whitish and slightly translucent appearance (E).

Fig. 2. Quantification of soluble proteins in the control and decell groups. Student´s t-distribution was applied to compare both groups (mean ± SD, **** $p \leq 0.0001$).

Fig. 3. Ovarian matrisome proteins. Core matrisome proteins (ECM glycoproteins (A), collagens (B), and proteoglycans (C)) and matrisome-associated proteins (ECM-affiliated proteins (D), ECM regulators (E), and secreted factors (F)) identified in the native (blue, control group) and decell bovine ovarian tissue (red, decell group) and quantified by abundance (mean ±SD). Student´s t-distribution (*$p \leq 0.05$, **$p \leq 0.01$, ***$p \leq 0.001$) was performed for the proteins present in both groups.

Fig. 4. Top 58 most abundant proteins. All samples of the native (blue, control group) and decell bovine ovarian tissue (red, decell group) were organized based on their peptide spectrum matches.

Fig. 5. Number of proteins identified in native (blue, control group) and decell bovine ovarian tissue (red, decell group). (A) Biological process, (B) cellular component, and (C) molecular function categories.

Fig. 6. Histological staining in the native (control group) and decell bovine ovarian tissue (decell group). (A,B) Hematoxylin-eosin, showing the general morphology of ECM. Inserts show a closer view of the tissue (Bar = 50μm). Arrows point to cellular nuclei. (C,D) Masson's trichrome, showing the collagen fibers (green) in both groups, demonstrating their conservation post-decellularization. (E,F). Alcian blue (pH 2.5), showing proteoglycans (blue) in both groups and showed their conservation post decellularization. Scale bar = 200μm.

Fig. 7. Immunohistochemical staining in native (control group) and decell bovine ovarian tissue (decell group). (A,B) Collagen type VI alpha 3 was selected as the most important proteins identified of the collagen group, and to confirm the proteomics result. (C,D) EMILIN-1, (E,F) fibrilin-1 and elastin (G,H), components of the ECM-glycoproteins, were selected to confirm the proteomics result. Scale bar = 200μm.

Graphical abstract

Highlights

- Proteomic analysis of bovine ovarian extracellular matrix pre- and post-decellularization
- A total of 155 proteins were identified in the bovine ovary's extracellular matrix
- The decellularization protocol caused loss of only 10 of the 155 native matrix proteins
- Decellularized matrix shows promise for ovarian tissue engineering applications

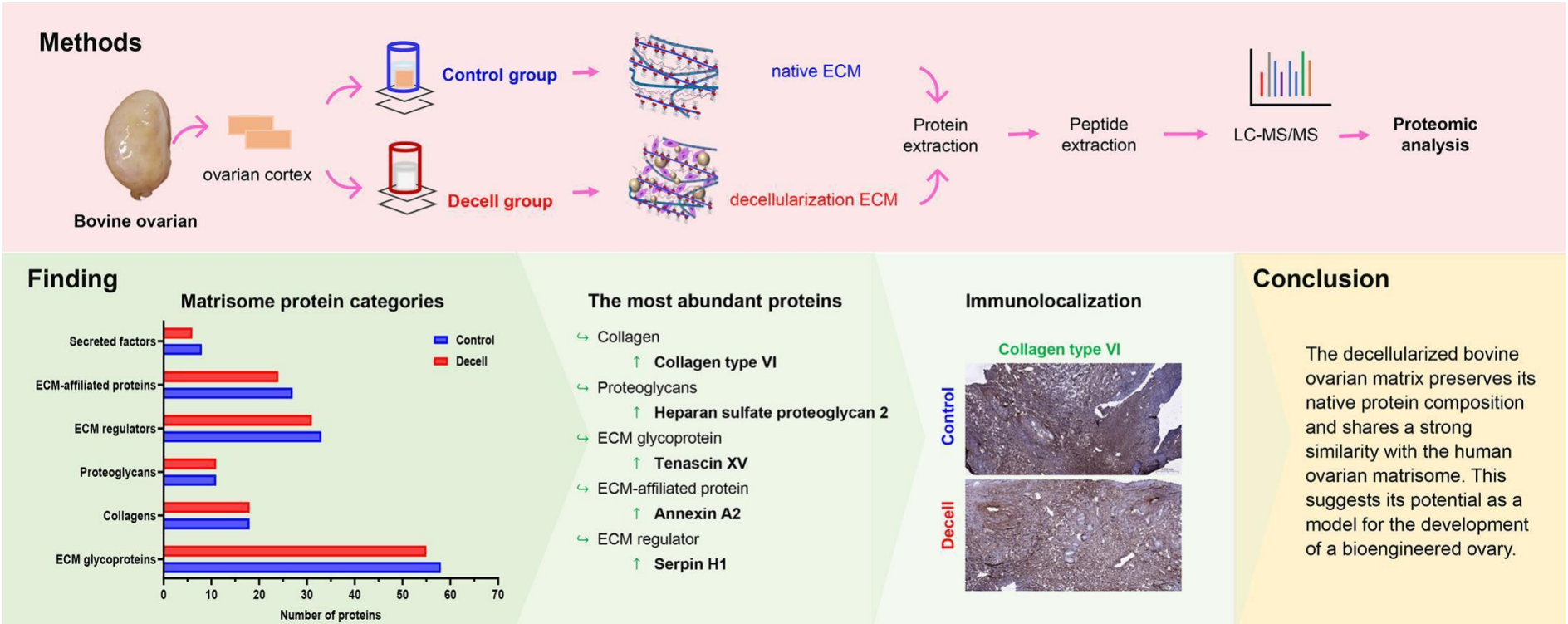

Graphics Abstract

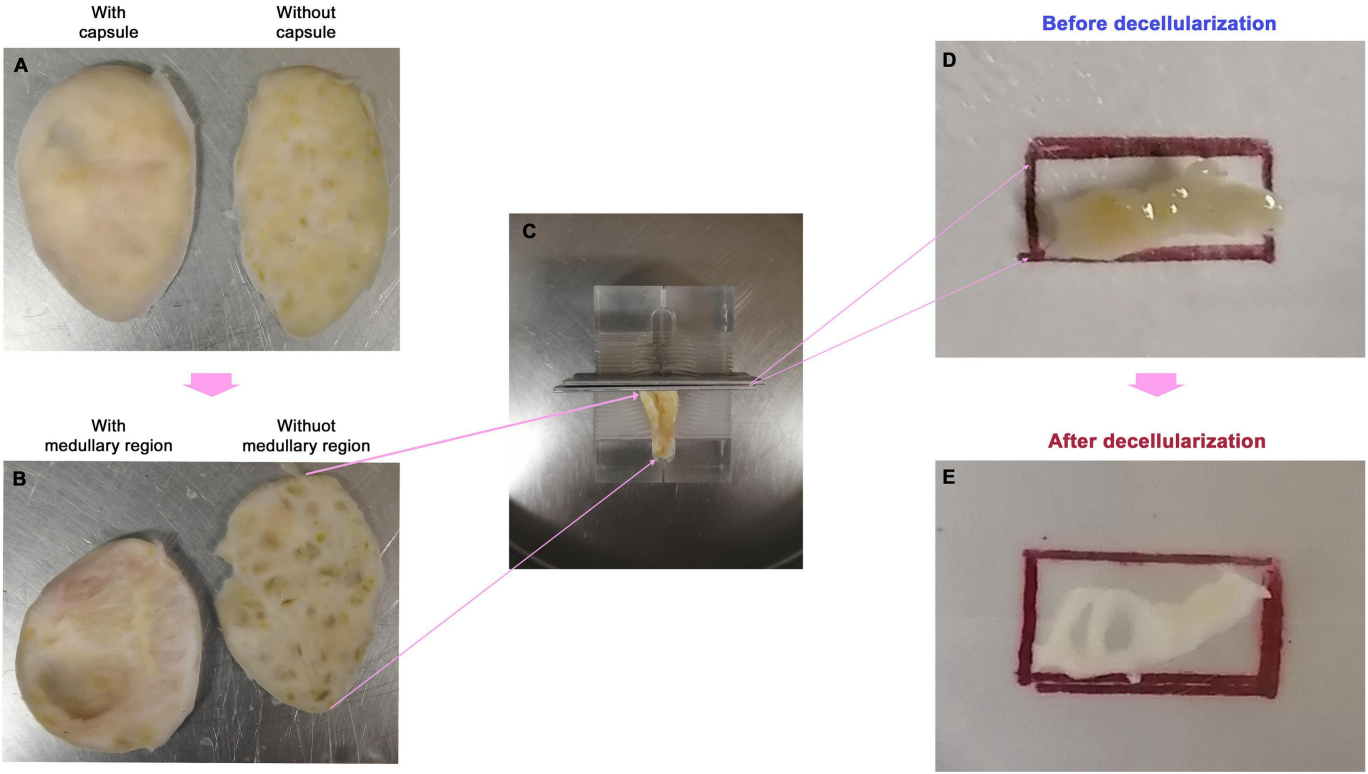
With capsule
Without capsule
A
With medullary region
Withuot medullary region
B
C
Before decellularization
D
After decellularization
E

Figure 1

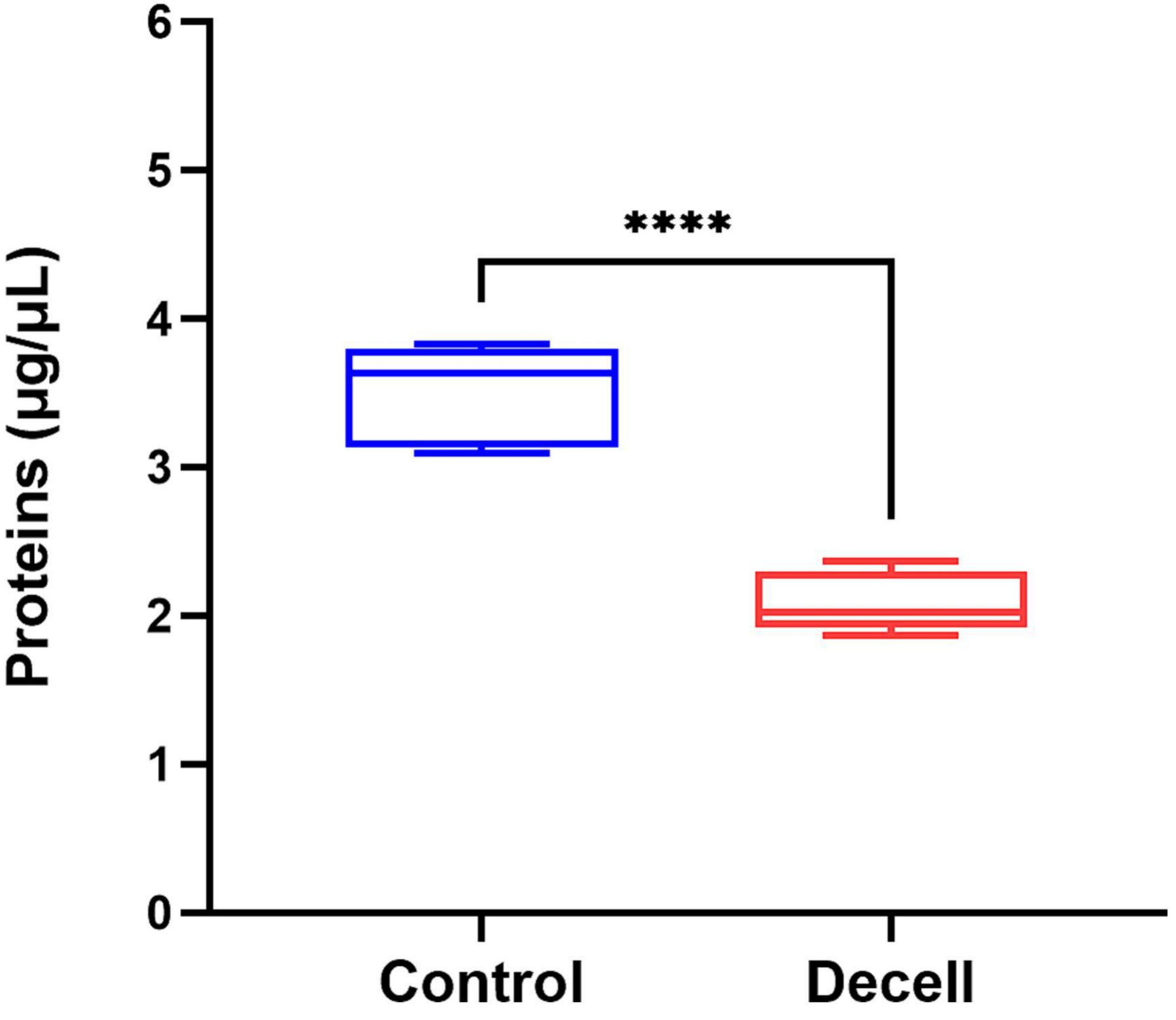

Figure 2

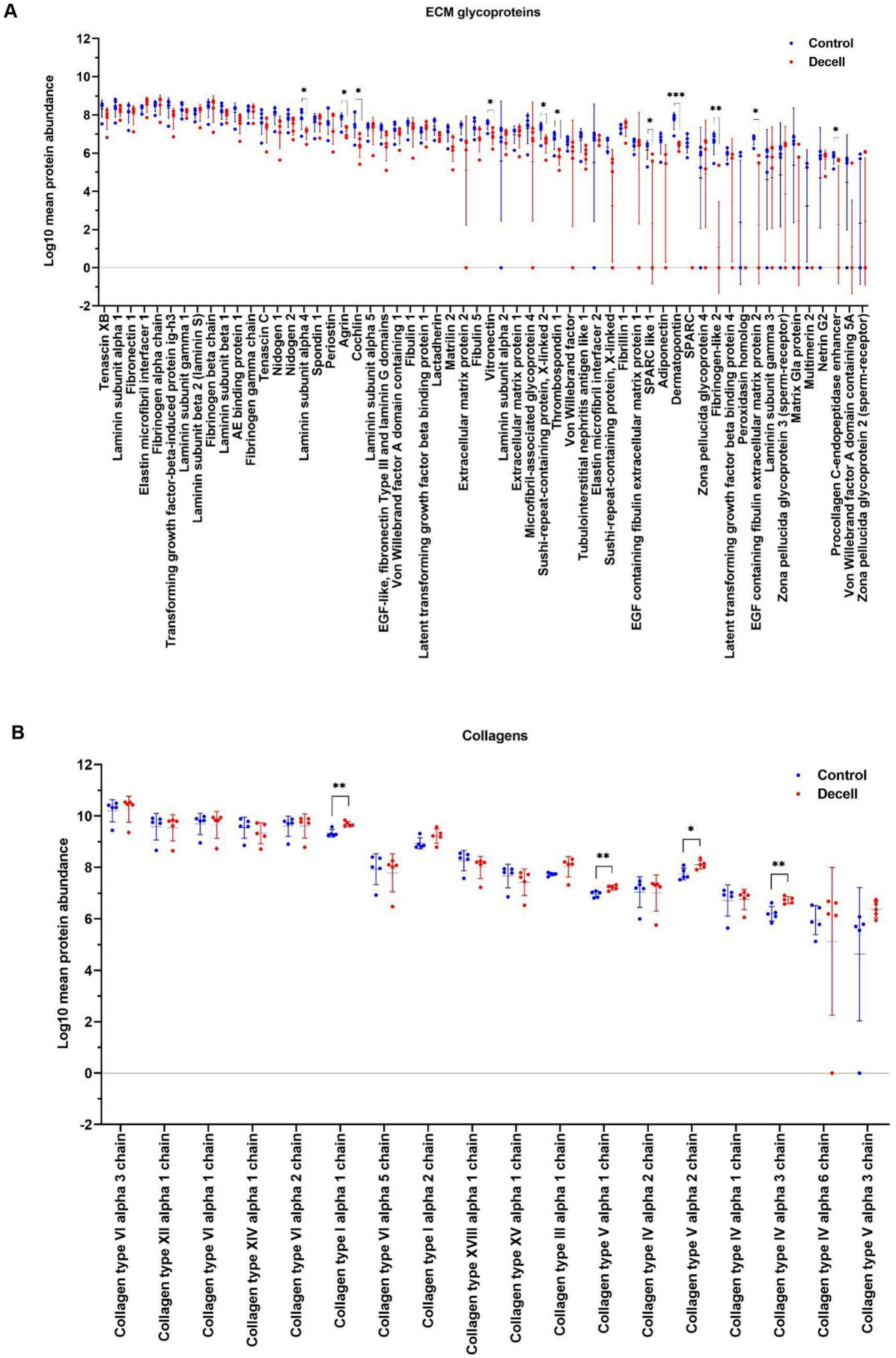
A
ECM glycoproteins
Control
Decell
Log10 mean protein abundance
12
10
8
6
4
2
0
-2
Tenascin XB
Laminin subunit alpha 1
Fibronectin 1
Elastin microfibril interfacer 1
Fibrinogen alpha chain
Transforming growth factor-beta-induced protein ig-h3
Laminin subunit gamma 1
Laminin subunit beta 2 (laminin S)
Fibrinogen beta chain
Laminin subunit beta 1
AE binding protein 1
Fibrinogen gamma chain
Tenascin C
Nidogen 1
Nidogen 2
Laminin subunit alpha 4
Spondin 1
Periostin
Agrin
Cochlin
Laminin subunit alpha 5
EGF-like, fibronectin Type III and laminin G domains
Von Willebrand factor A domain containing 1
Fibulin 1
Latent transforming growth factor beta binding protein 1
Lactadherin
Matrilin 2
Extracellular matrix protein 2
Fibulin 5
Vitronectin
Laminin subunit alpha 2
Extracellular matrix protein 1
Microfibril-associated glycoprotein 4
Sushi-repeat-containing protein, X-linked 2
Thrombospondin 1
Von Willebrand factor
Tubulointerstitial nephritis antigen like 1
Elastin microfibril interfacer 2
Sushi-repeat-containing protein, X-linked
Fibrillin 1
EGF containing fibulin extracellular matrix protein 1
SPARC like 1
Adiponectin
Dermatopontin
SPARC
Zona pellucida glycoprotein 4
Fibrinogen-like 2
Latent transforming growth factor beta binding protein 4
Peroxidasin homolog
EGF containing fibulin extracellular matrix protein 2
Laminin subunit gamma 3
Zona pellucida glycoprotein 3 (sperm-receptor)
Matrix Gla protein
Multimerin 2
Netrin G2
Procollagen C-endopeptidase enhancer
Von Willebrand factor A domain containing 5A
Zona pellucida glycoprotein 2 (sperm-receptor)
B
Collagens
Control
Decell
Log10 mean protein abundance
12
10
8
6
4
2
0
-2
Collagen type VI alpha 3 chain
Collagen type XII alpha 1 chain
Collagen type VI alpha 1 chain
Collagen type XIV alpha 1 chain
Collagen type VI alpha 2 chain
Collagen type I alpha 1 chain
Collagen type VI alpha 5 chain
Collagen type I alpha 2 chain
Collagen type XVIII alpha 1 chain
Collagen type XV alpha 1 chain
Collagen type III alpha 1 chain
Collagen type V alpha 1 chain
Collagen type IV alpha 2 chain
Collagen type V alpha 2 chain
Collagen type IV alpha 1 chain
Collagen type IV alpha 3 chain
Collagen type IV alpha 6 chain
Collagen type V alpha 3 chain

Figure 3A

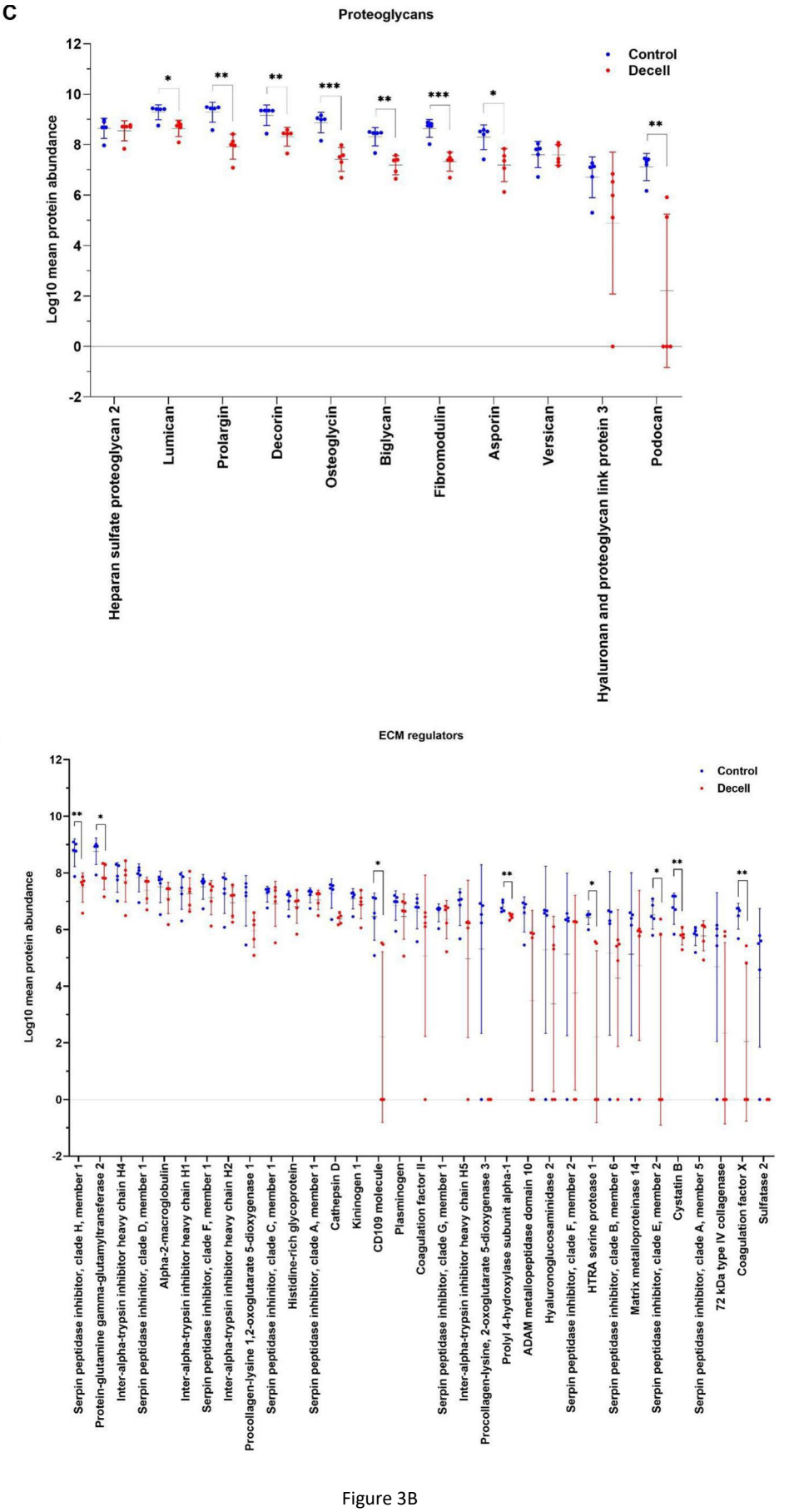
C
Proteoglycans
Control
Decell
Log10 mean protein abundance
12
10
8
6
4
2
0
-2
*
**
**
***
**
***
*
**
Heparan sulfate proteoglycan 2
Lumican
Prolargin
Decorin
Osteoglycin
Biglycan
Fibromodulin
Asporin
Versican
Hyaluronan and proteoglycan link protein 3
Podocan
D
ECM regulators
Control
Decell
Log10 mean protein abundance
12
10
8
6
4
2
0
-2
**
*
*
**
*
**
**
Serpin peptidase inhibitor, clade H, member 1
Protein-glutamine gamma-glutamyltransferase 2
Inter-alpha-trypsin inhibitor heavy chain H4
Serpin peptidase inhinitor, clade D, member 1
Alpha-2-macroglobulin
Inter-alpha-trypsin inhibitor heavy chain H1
Serpin peptidase inhibitor, clade F, member 1
Inter-alpha-trypsin inhibitor heavy chain H2
Procollagen-lysine 1,2-oxoglutarate 5-dioxygenase 1
Serpin peptidase inhinitor, clade C, member 1
Histidine-rich glycoprotein
Serpin peptidase inhibitor, clade A, member 1
Cathepsin D
Kininogen 1
CD109 molecule
Plasminogen
Coagulation factor II
Serpin peptidase inhibitor, clade G, member 1
Inter-alpha-trypsin inhibitor heavy chain H5
Procollagen-lysine, 2-oxoglutarate 5-dioxygenase 3
Prolyl 4-hydroxylase subunit alpha-1
ADAM metallopeptidase domain 10
Hyaluronoglucosaminidase 2
Serpin peptidase inhibitor, clade F, member 2
HTRA serine protease 1
Serpin peptidase inhibitor, clade B, member 6
Matrix metalloproteinase 14
Serpin peptidase inhibitor, clade E, member 2
Cystatin B
Serpin peptidase inhibitor, clade A, member 5
72 kDa type IV collagenase
Coagulation factor X
Sulfatase 2

Figure 3B

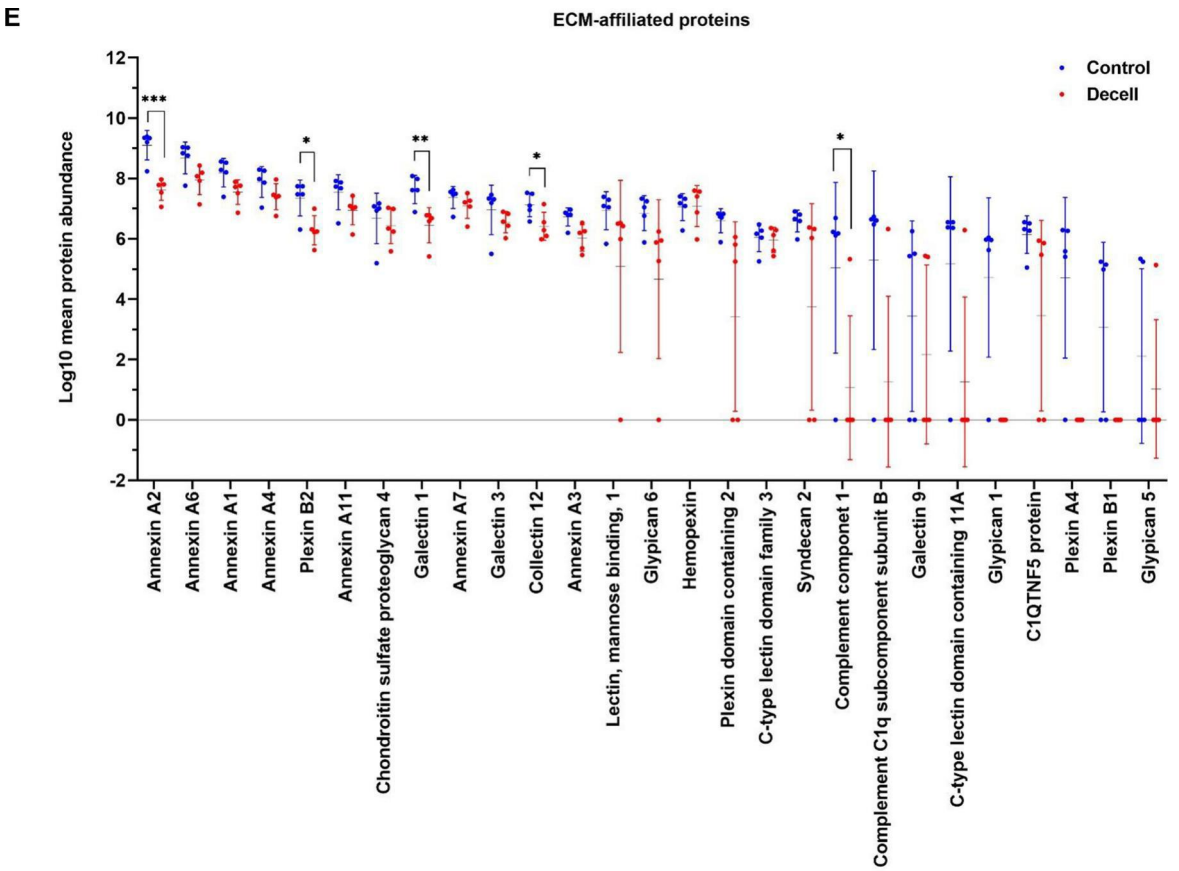
E
ECM-affiliated proteins
Control
Decell
Log10 mean protein abundance
12
10
8
6
4
2
0
-2
***
*
**
*
*
Annexin A2
Annexin A6
Annexin A1
Annexin A4
Plexin B2
Annexin A11
Chondroitin sulfate proteoglycan 4
Galectin 1
Annexin A7
Galectin 3
Collectin 12
Annexin A3
Lectin, mannose binding, 1
Glypican 6
Hemopexin
Plexin domain containing 2
C-type lectin domain family 3
Syndecan 2
Complement componet 1
Complement C1q subcomponent subunit B
Galectin 9
C-type lectin domain containing 11A
Glypican 1
C1QTNF5 protein
Plexin A4
Plexin B1
Glypican 5

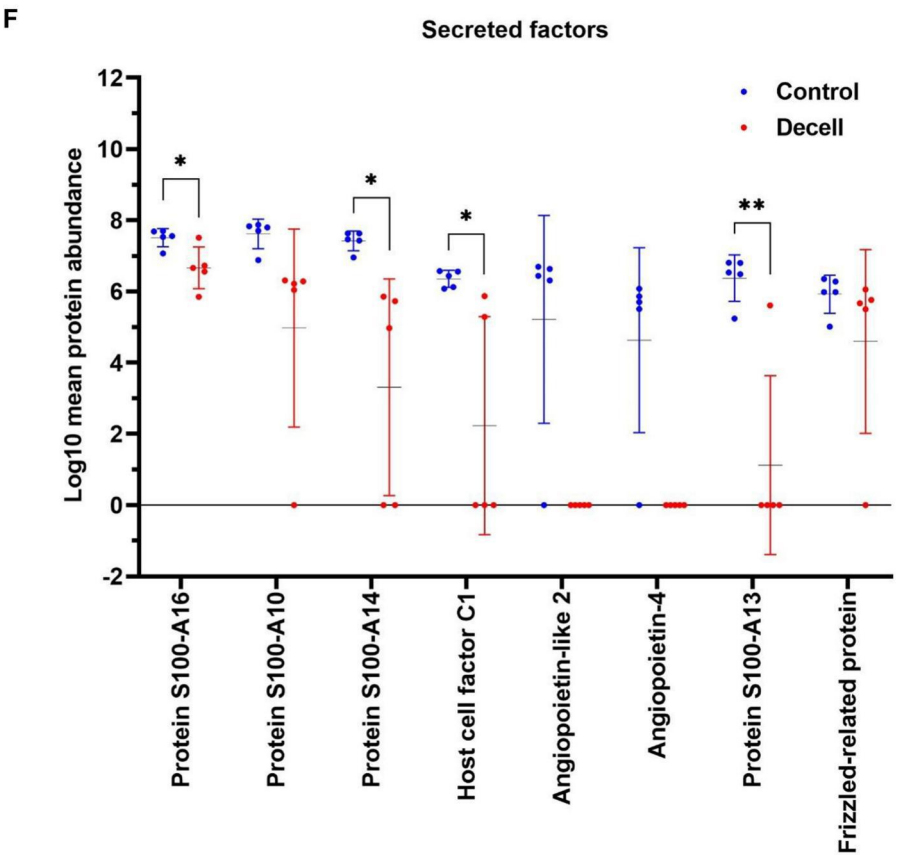
F
Secreted factors
Control
Decell
Log10 mean protein abundance
12
10
8
6
4
2
0
-2
*
*
*
**
Protein S100-A16
Protein S100-A10
Protein S100-A14
Host cell factor C1
Angiopoietin-like 2
Angiopoietin-4
Protein S100-A13
Frizzled-related protein

Figure 3C

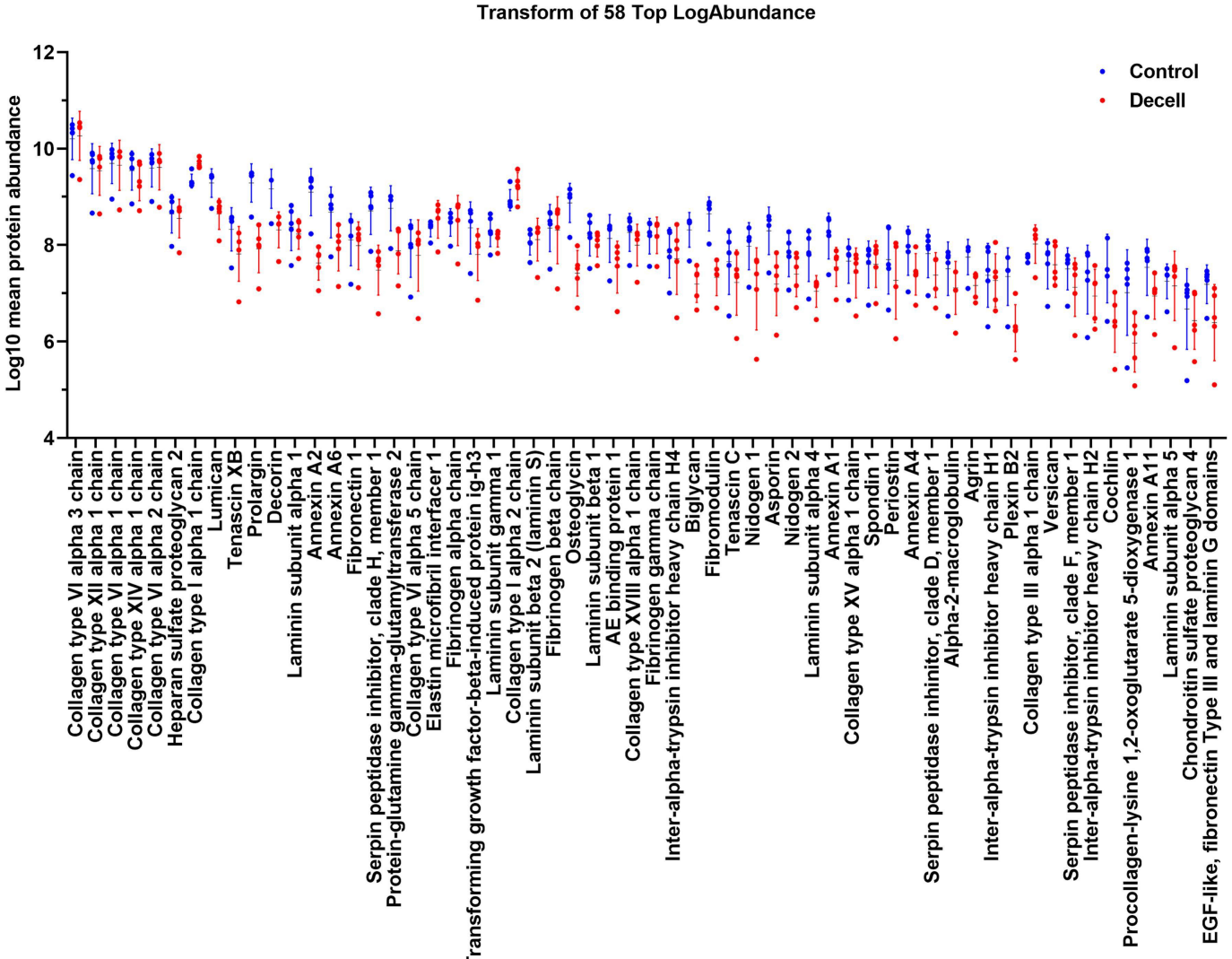
Transform of 58 Top LogAbundance
Log10 mean protein abundance
12
10
8
6
4
Control
Decell
Collagen type VI alpha 3 chain
Collagen type XII alpha 1 chain
Collagen type VI alpha 1 chain
Collagen type XIV alpha 1 chain
Collagen type VI alpha 2 chain
Heparan sulfate proteoglycan 2
Collagen type I alpha 1 chain
Lumican
Tenascin XB
Prolargin
Decorin
Laminin subunit alpha 1
Annexin A2
Annexin A6
Fibronectin 1
Serpin peptidase inhibitor, clade H, member 1
Protein-glutamine gamma-glutamyltransferase 2
Collagen type VI alpha 5 chain
Elastin microfibril interfacer 1
Fibrinogen alpha chain
Transforming growth factor-beta-induced protein ig-h3
Laminin subunit gamma 1
Collagen type I alpha 2 chain
Laminin subunit beta 2 (laminin S)
Fibrinogen beta chain
Osteoglycin
Laminin subunit beta 1
AE binding protein 1
Collagen type XVIII alpha 1 chain
Fibrinogen gamma chain
Inter-alpha-trypsin inhibitor heavy chain H4
Biglycan
Fibromodulin
Tenascin C
Nidogen 1
Asporin
Nidogen 2
Laminin subunit alpha 4
Annexin A1
Collagen type XV alpha 1 chain
Spondin 1
Periostin
Annexin A4
Serpin peptidase inhinitor, clade D, member 1
Alpha-2-macroglobulin
Agrin
Inter-alpha-trypsin inhibitor heavy chain H1
Plexin B2
Collagen type III alpha 1 chain
Versican
Serpin peptidase inhibitor, clade F, member 1
Inter-alpha-trypsin inhibitor heavy chain H2
Cochlin
Procollagen-lysine 1,2-oxoglutarate 5-dioxygenase 1
Annexin A11
Laminin subunit alpha 5
Chondroitin sulfate proteoglycan 4
EGF-like, fibronectin Type III and laminin G domains

Figure 4

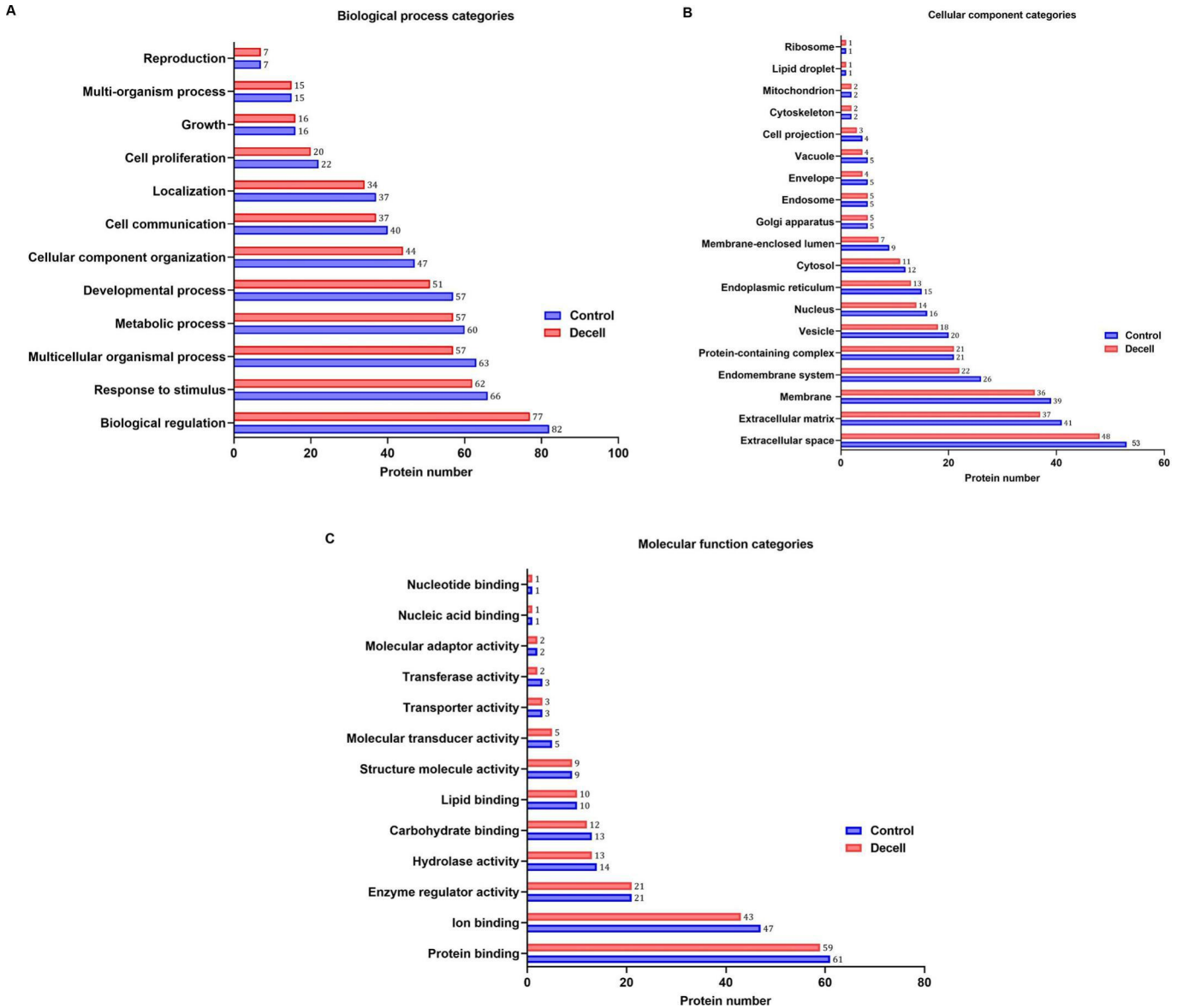
A
Biological process categories
Reproduction
Multi-organism process
Growth
Cell proliferation
Localization
Cell communication
Cellular component organization
Developmental process
Metabolic process
Multicellular organismal process
Response to stimulus
Biological regulation
7
7
15
15
16
16
20
22
34
37
37
40
44
47
51
57
57
60
57
63
62
66
77
82
Control
Decell
0
20
40
60
80
100
Protein number
B
Cellular component categories
Ribosome
Lipid droplet
Mitochondrion
Cytoskeleton
Cell projection
Vacuole
Envelope
Endosome
Golgi apparatus
Membrane-enclosed lumen
Cytosol
Endoplasmic reticulum
Nucleus
Vesicle
Protein-containing complex
Endomembrane system
Membrane
Extracellular matrix
Extracellular space
1
1
1
1
2
2
2
2
3
4
4
5
4
5
5
5
5
5
7
9
11
12
13
15
14
16
18
20
21
21
22
26
36
39
37
41
48
53
Control
Decell
0
20
40
60
Protein number
C
Molecular function categories
Nucleotide binding
Nucleic acid binding
Molecular adaptor activity
Transferase activity
Transporter activity
Molecular transducer activity
Structure molecule activity
Lipid binding
Carbohydrate binding
Hydrolase activity
Enzyme regulator activity
Ion binding
Protein binding
1
1
1
1
2
2
2
3
3
3
5
5
9
9
10
10
12
13
13
14
21
21
43
47
59
61
Control
Decell
0
20
40
60
80
Protein number

Figure 5

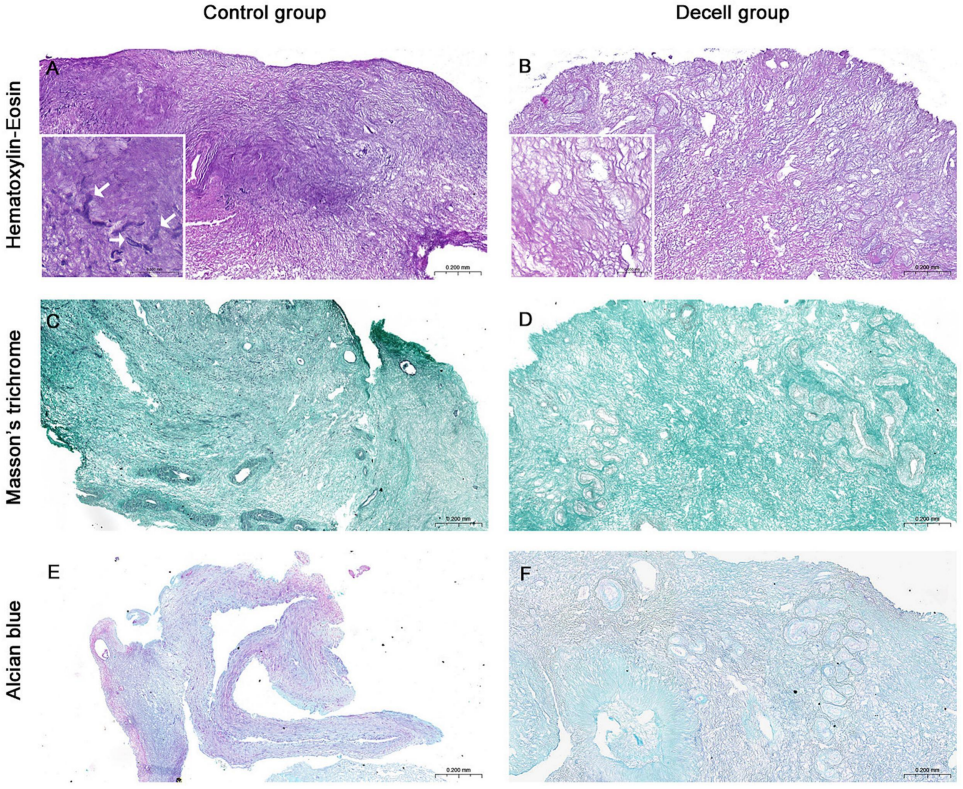
Control group
Decell group
Hematoxylin-Eosin
Masson's trichrome
Alcian blue
A
B
C
D
E
F

Figure 6

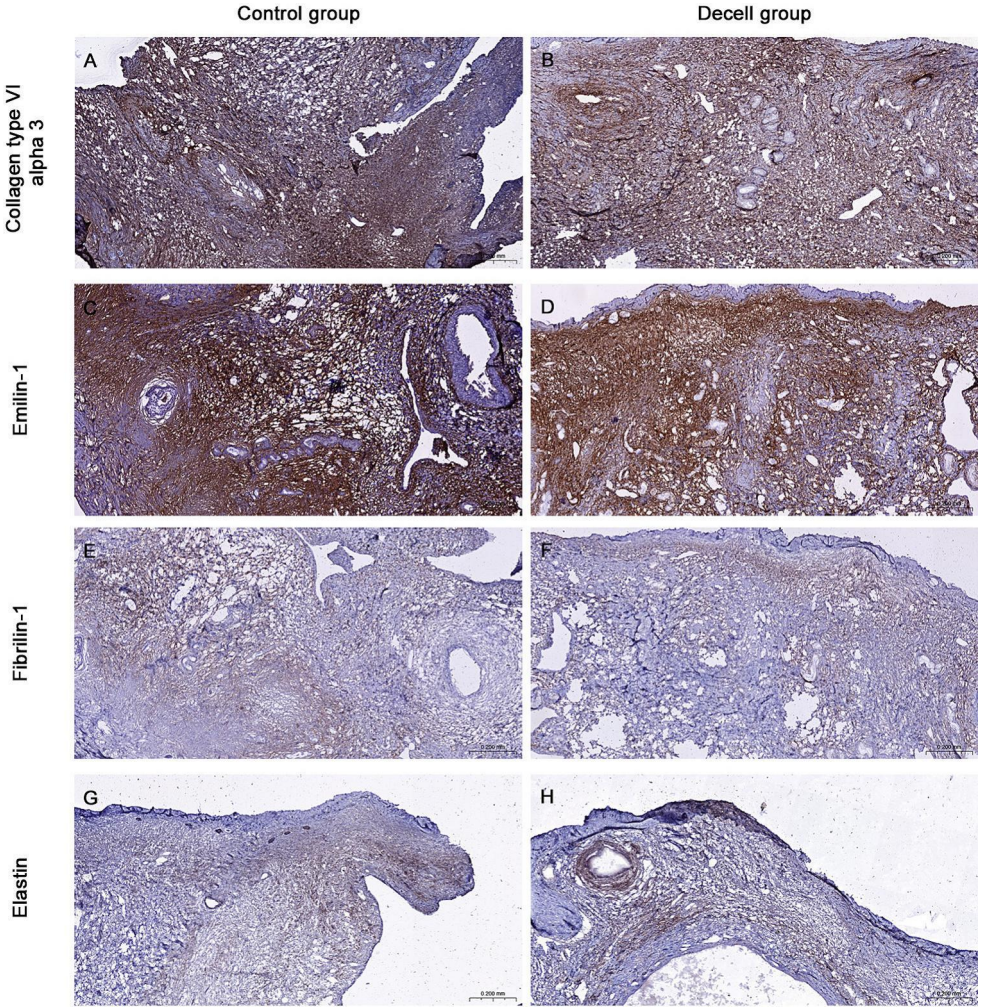
Control group
Decell group
Collagen type VI alpha 3
Emilin-1
Fibrilin-1
Elastin
A
B
C
D
E
F
G
H

Figure 7